RELATIVE TRANSITION PROBABILITIES OF THE CN VIOLET BAND SYSTEM FROM BAND HEAD DATA

Thesis by

Acey L. Floyd

In Partial Fulfillment of the Requirements

for the Degree of

Doctor of Philosophy

California Institute of Technology

Pasadena, California

1954

ACKNOWLEDGEMENTS

The need for relative vibrational transition probabilities of the CN violet band system was pointed out by Dr. P. Swings and Dr. R. B. King. My sincere thanks are due to Professor King who, from the time of the assignment of the research to its completion, gave the advice, the aid, and the encouragement that were necessary in the solution of the many problems encountered while performing the research. I wish to thank my sister, Mrs. H. Fredregill who very carefully and conscientiously typed the thesis.

ABSTRACT

The relative vibrational transition probabilities of the first four bands in the sequences $\Delta v = -1, 0, +1$ of the violet CN system ($^2\Sigma - {}^2\Sigma$) have been calculated using the Morse potential function. The same relative vibrational transition probabilities were derived from peak relative intensities of the band heads appearing in the electric furnace emission spectrum under conditions approaching thermodynamic equilibrium. The calculated and measured relative vibrational transition probabilities were compared and shown to agree within the limit of accuracy of the experiment and of the calculations.

TABLE OF CONTENTS

INTRODUCTION

The violet CN bands, arising from a $^2\Sigma - ^2\Sigma$ electronic transition, are well known and are emitted by most spectral sources containing carbon. For this reason the use of CN band intensity data for determining temperature has gradually come into wide use. Where it has been practical, temperature has been determined from the rotational structure within the bands. However, in many cases, as in faint stars, it is not practical to use high dispersion spectrographs required to resolve the rotational structure. For these cases the relative intensities of the band heads are used. The use of band head intensities requires a knowledge of the relative vibrational transition probabilities of the band heads and the manner in which their relative intensities vary with temperature.

The relative vibrational transition probabilities of the CN violet bands have been determined by Brinkman[1], with the aid of the "sum rule" for band spectra, from measurements of the intensities of these bands in the spectrum of the carbon arc. Later, his results for the first two bands in the $\Delta v=-1$ sequence and the $\Delta v=0$ sequence were used by Smit-Miessen and Spiers[2,3] to construct graphs of relative intensities for pairs of these band heads vs temperature. Smit-Miessen and Spiers used the established theoretical formulas for the relative intensities of the rotational lines within the bands, assumed certain line widths, rectangular line shapes, and integrated to obtain the unresolved band

shapes at various temperatures. In this manner plots of intensity ratios of the (1-1) to the (0-0) and of the (0-1) to the (1-2) bands as a function of temperature were developed. Smit-Miessen and Spiers' calculations were long and involved. Their results varied if they altered some of the arbitrary factors in their calculations, such as the line widths. Their results also depended directly upon the transition probabilities measured by Brinkman. However Brinkman's measurements were made on the spectrum of the carbon arc where the temperature could not be accurately determined by independent means. For these reasons Smit-Miessen and Spiers stated that their results should be checked under conditions where the temperature could be determined independently.

The present investigation of the CN violet band system was therefore initiated in order to:

(a) Examine the reliability of determining temperature from band head intensity measurements, particularly when the band heads belong to different sequences.

(b) Increase the number of band heads that can be used for temperature determination.

(c) Determine if theoretical vibrational transition probabilities of the CN violet band system, calculated by means of the "over-lap integrals"[4], can be used for accurate temperature determination when experimental values are not available.

The electric furnace developed by King[5] provides an

excellent device for investigating the CN violet band system and was used in this experiment. In such a furnace the spectra of atoms or molecules can be excited under conditions approximating thermal equilibrium over a wide range of known and controllable temperatures.

This investigation was carried out in the following manner:

(a) Calculate the relative transition probabilities as accurately as possible for those CN violet bands whose intensities can be accurately measured in electric furnace spectra.

(b) Measure the relative transition probabilities of the CN violet bands in the electric furnace, making the measurements of the band head intensities by a method that can be used for temperature determination with a low dispersion spectrograph.

If the theoretical and experimental values for the relative transition probabilities agree, then it should be reasonable to conclude that all the bands measured can be used for reliable temperature determination. Agreement would also indicate that calculated relative transition probabilities for similar bands for which experimental data are not available might be used with considerable confidence.

II. CALCULATION OF RELATIVE TRANSITION PROBABILITIES

General Considerations

Relative vibrational transition probabilities for molecules can be calculated with the aid of the Frank-Condon Principle. This principle is that during an electronic transition the relative position of the atomic nuclei in a molecule does not change. Consequently for a molecule whose electric moment does not vary with relative position of the nuclei, and for which the vibrational part of the wave function for the molecule can be separated, the relative transition probabilities are given by[4]

$$R^2_{v'v''} = \bar{R}^2_e \left[\int_0^\infty \psi'_{v'} \cdot \psi''_{v''} \, dr \right]^2 \qquad (1)$$

where $\psi'_{v'}$ is the vibrational eigenfunction of the upper energy level with vibrational quantum number v', $\psi''_{v''}$ is the vibrational eigenfunction of the lower state with vibrational quantum number v'', $\bar{R}^2_e$ is a constant, and $R^2_{v'v''}$ is the relative transition probability. Usually the transition between the two lowest vibrational states, the 0-0 transition, is taken as a reference, and the relative vibrational transition probabilities are given by

$$R^2_{v'v''} = \left[\frac{\int_0^\infty \psi'_{v'} \cdot \psi''_{v''} \, dr}{\int_0^\infty \psi'_0 \cdot \psi''_0 \, dr} \right]^2 \qquad (2)$$

Thus, to calculate the relative transition probabilities it is necessary only to evaluate the integral of the product of the wave function of the two vibrational states involved, the so called "over-lap integral". While in principle this is simple, the actual mechanics of determining the wave functions and evaluating the integrals is complicated by the difficulty of obtaining a suitable analytical representation for the variation of potential energy with internuclear distance for diatomic molecules. Hutchisson[6], using the harmonic oscillator potential function, has developed formulas for the vibrational transition probabilities for homonuclear diatomic molecules. However the agreement between values calculated from these formulas and values obtained from experimental data has been only fair. Later, Hutchisson[7], using first order perturbation theory, extended these formulas to include some of the anharmonic effect of diatomic molecular vibrations. These formulas are quite complicated and little use has been made of them.

If more accurate calculations of the transition probabilities are to be carried out for purposes of this investigation, several possibilities are open. The perturbation calculations carried out by Hutchisson could be extended to include second order terms and thus increase the accuracy. However, as the first order perturbation formulas for relative intensity are so complicated as to seriously limit their use, the second order formulas would be even more involved and still less practical to use. Therefore, the second order approximation does not appear to offer a practical

approach to the problem. The useful Wentzel-Kramer-Brillouion[8] approximation offers another possibility. It has been shown that the maximum contribution to the probability of a given vibrational transition occurs in the region corresponding to the classical turning point of the molecular vibration. This gives rise to the familiar intensity parabolas[9]. However it is in this region that the Wentzel-Kramer-Brillouion approximation is the least accurate. Therefore, its use would not be expected to yield transition probabilities of the desired accuracy.

The next choice is to investigate the use of the wave functions obtained from the Morse potential function[10]. These wave functions give vibrational energy levels which are more accurate than those given by second order perturbation calculations and which agree with measured values for the CN violet band system within the errors of measurement. Therefore, the possibility of using these wave functions for vibrational transition probability calculations will be investigated. The Morse potential function is of the form

$$U(r-r_e) = D_e\left(1-e^{-a(r-r_e)}\right)^2 \qquad (3)$$

where r is the internuclear distance, r_e is the equilibrium internuclear distance, and a and D_e are constants that depend on the electronic state of the molecule, and are in general different for each electronic state. The wave equation has been solved many times for this potential function[11]. Letting

$$y = e^{-a(r-r_e)} \tag{4}$$

Schrodinger's equation becomes

$$\frac{1}{Y}\frac{d}{dY}\left(Y\frac{d\psi}{dY}\right) + \frac{8\pi^2\mu}{a^2h^2}\left(\frac{E-D_e}{Y^2} + \frac{2D_e}{Y} - D_e\right)\psi = 0$$

where μ is the reduced mass, h is Planck's constant, and E is the energy of vibration. Now, following Wu[11]; let

$$\psi = N e^{-\frac{z}{2}} z^{\frac{\beta}{2}} F(z) \tag{5}$$

where

$$z = 2\alpha Y \;, \qquad \alpha = \frac{2\pi\sqrt{2\mu D_e}}{a h} \;,$$

$$E - D_e = -\frac{a^2h^2\beta^2}{32\pi^2\mu} \;, \qquad N = \text{normalization coefficient} \tag{6}$$

and the equation for $F(z)$ is

$$zF''(z) + (\beta+1-z)F'(z) + \tfrac{1}{2}(2\alpha-\beta-1)F(z) = 0$$

This equation is to be solved by series. However, as the series diverges for large z, suitable values for β must be chosen so that the series terminates, in order to obtain satisfactory solutions to the wave equation. Letting

$$F(z) = \sum C_n z^n$$

the recursion formula for the C_n becomes

$$C_{n+1} = \frac{n - \frac{1}{2}(2\alpha - \beta - 1)}{(n+1)n - (n+1)(\beta+1)} C_n \qquad (7)$$

Thus, if the series is to terminate at some value of n, the suitable values of β_n are

$$\beta_n = 2\alpha - 1 - 2n$$

giving eigenvalues of E by Equation (6)

$$E_n - D_e = -\frac{a^2 h^2}{32\pi^2 \mu} (2\alpha - 1 - 2n)^2 \qquad (8)$$

or

$$E_n = \frac{a^2 h^2 \alpha}{4\pi\mu}(n+\tfrac{1}{2}) - \frac{a^2 h^2}{8\pi^2 \mu}(n+\tfrac{1}{2})^2$$

$$= ch\omega_e (n+\tfrac{1}{2}) - ch\omega_e x_e (n+\tfrac{1}{2})^2 \qquad (9)$$

where ω_e is the vibrational wave number in cm^{-1} and $\omega_e x_e$ is a correction term for anharmonic effects. Since ω_e and $\omega_e x_e$ can be determined very accurately from wave length measurements, the values of D_e and a can be calculated. In particular

$$D_e = hc\frac{\omega_e^2}{4\omega_e x_e} = \frac{\omega_e^2}{4\omega_e x_e}\ cm^{-1} \tag{10}$$

$$a = 2.4354\times 10^7\sqrt{\mu_A \omega_e x_e}\ cm^{-1} \tag{11}$$

where μ_A is in Aston units.

The normalization coefficients are determined in the usual way from

$$N_n^2\int_o^\infty (\psi_n(r))^2 dr = \frac{N_n^2}{a}\int_o^\infty (\psi_n(z))^2\frac{dz}{z} = 1$$

giving

$$N_n^2 = \frac{a[2\alpha-(n+1)]\cdot\cdot\cdot\cdot[2\alpha-2n]}{n!\,\Gamma(2\alpha-2n-1)}\ . \tag{12}$$

In principle these solutions to the wave equation may now be used to calculate the "over-lap integrals". But as D_e and a are different for different electronic states, the value of z' for one electronic state as a function of z'' for another, say the ground state, is of the form

$$z' = K(z'')^\gamma$$

by the definition of z from Equations (6) and (4). The exponent γ differs from unity except when the values of a for the two electronic states involved are identical. In general these are different and the "over-lap integrals" take the form, by Equations (1) and (5),

$$\int_0^\infty C\, e^{\frac{z}{2} + \frac{Kz^\gamma}{2}} P(z)\, dz \qquad (13)$$

where C , K and γ are constants and $P(z)$ is a polynomial in z . This integral can not be evaluated in terms of simple functions unless γ is unity, that is, unless the value of a for the two electronic states involved is the same.

Approximate Representation of the Wave Functions

Examination of Equation (13) indicates that the"over-lap integrals" could be evaluated in terms of the gamma function if the value of γ happened to be unity. The Morse potential function, Equation (3), shows that a acts as a scale factor for r and D_e acts as a scale factor for $U(r-r_e)$. Therefore one might expect that for low energy states the wave functions should be represented almost exactly by those obtained from a potential function chosen in the following manner.

1. Choose a so that the "over-lap integrals" can be evaluated.

2. Offset the effect of the error in a by choosing a new scale factor D_e such that the width of the potential function at the energy levels of interest is the same as that for the true Morse potential function.

3. Vary the value of r_e , the equilibrium position, with each energy level so that the new potential function matches the true Morse potential function at the energy state involved.

In view of the classical relation between amplitude of vibration of an oscillator and the width of the potential

function, this method of obtaining wave functions will be referred to as an equal amplitude approximation.

This equal amplitude approximation will now be used to construct a potential function for the upper $^2\Sigma^+$ state of CN. The values of ω_e and $\omega_e x_e$ given in Table I are taken from Herzberg[12] and D_e and a are calculated by Equations (10) and (11). State B is the excited electronic state and state X the ground electronic state, transitions between which give rise to the violet CN bands.

TABLE I

Vibrational Constants of CN

STATE	ω_e (cm^{-1})	$\omega_e x_e$ (cm^{-1})	r_e (Å)	D_e (cm^{-1})	a ($Å^{-1}$)
B	2164.13	20.25	1.1506	57820.47	2.7864
X	2068.705	13.144	1.1718	81397.23	2.2449

With these constants the Morse potential function for the excited CN state (B) becomes

$$U(r-r_e) = 57,820.48\left[1 - e^{-2.7864(r-1.1506)}\right]^2 .$$

An accurate plot of this potential function is shown by the solid line in Figure 1. To obtain the first approximation to this potential by a potential function which has an a of 2.2449 $Å^{-1}$, as for the ground state, the potential function is expanded in a series as follows:

$$U(r-r_e') = D_e'\left[1-e^{-a'(r-r_e')}\right]^2 \approx D_e'\left[a'(r-r_e')+\cdots\right]^2$$

$$\approx D_e'\left[\frac{a'}{a''}\right]^2\left[a''(r-r_e')+\cdots\right]^2 \approx D_e'\left[\frac{a'}{a''}\right]^2\left[1-e^{-a''(r-r_e')}\right]^2 .$$

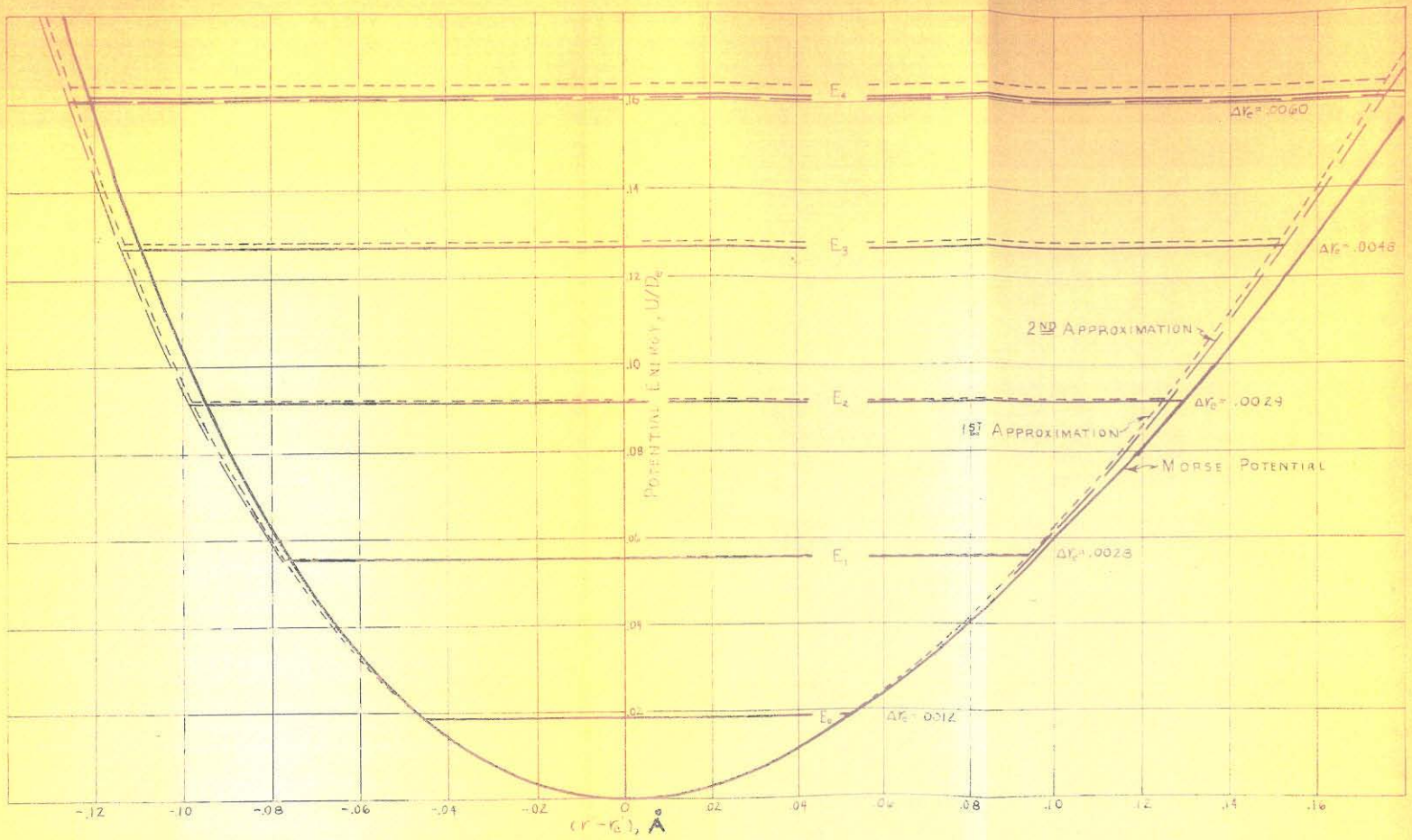

FIGURE 1

APPROXIMATE POTENTIAL FUNCTIONS FOR THE EXCITED $^2\Sigma$ STATE OF CN

Thus,

$$U_{(1)}(r-r_e') = 57,820.48\left[\frac{2.7864}{2.2449}\right]^2\left[1 - e^{-2.2449(r-1.1506)}\right]^2 .$$

Thus, the first approximation to the new dissociation energy to be used to offset the error in a is

$$D_{e(1)}' = 89,079.77 \ cm^{-1} .$$

The approximate potential function is plotted by the dotted line in Figure 1. It can be seen from Figure 1 that the widths of the two potentials at the energy levels are almost the same. However, for all energy levels considered here the deviation in width of the approximate potential is negative, and the deviation in energy of the energy levels is positive.

A further change in $D_{e(1)}'$ should give a little better approximation to equal widths at the energy levels over the range plotted for the two potentials. However, it must be noted that the positions of the energy levels shift when $D_{e(1)}$ is changed. Fortunately, these shifts are such as to tend to keep the widths of the two potential functions equal at the corresponding energy levels. Thus matching the width at the energy level E_3 should give an accurate match for the other energy levels shown on Figure 1. In Figure 1 the solid horizontal line labeled E_3 represents the true Morse energy level; the dotted line above it represents the energy level for the first approximation.

Since the second variation in D_e' is to be small, the variation in width of the potential function with energy can be considered as linear in the region of E_3 . That is

$$\Delta W = \Delta E \frac{K}{D_e'}$$

where ΔW is the change in width, ΔE is the change in energy and $\frac{K}{D_e'}$ is a constant. Therefore, if the dissociation energy is changed by

$$\Delta D_{e(1)}' = -(1-f^2) D_{e(0)}' \quad , \quad |1-f^2| << 1 \quad ,$$

the change in energy at the energy level is

$$\Delta E = (1-f^2) U_{(1)}(r-r_e') \quad .$$

The change in width at the energy level is

$$\Delta W = (1-f^2) \frac{K}{D_e'} U_{(1)}(r-r_e') \quad .$$

However the positions of the energy levels have shifted. By Equation (11), $\omega_e x_e$ remains constant as the value of α has not been changed, therefore

$$\Delta E = -(1-f)(n+\tfrac{1}{2}) \omega_e' \quad , \quad 1 > f > 0 \quad .$$

Thus the change in width associated with the shift in energy level is

$$\Delta W = -(1-f)(n+\tfrac{1}{2}) \omega_e' \frac{K}{D_e'} \quad .$$

The total change in width is

$$\Delta W_T = \left[(1-f^2) U_{(1)}(r-r_e') - (1-f)(n+\tfrac{1}{2}) \omega_e'\right] \frac{K}{D_e'} \quad . \qquad (14)$$

However, the value of $U_{(1)}(r-r_e')$ is the same as that of the energy level involved; thus Equation (14) becomes

$$\frac{\Delta W}{(n+\frac{1}{2})\omega_e' \frac{K}{D_e}} = -f^2 + f$$

Solving for f :

$$f = \frac{1}{2}\left(1 + \sqrt{1 - \frac{4\Delta W}{(n+\frac{1}{2})\omega_e' \frac{K}{D_e'}}}\right) \approx 1 - \frac{\Delta W}{(n+\frac{1}{2})\omega_e' \frac{K}{D_e'}} \quad . \qquad (15)$$

The desired change in width at energy level E_3 , which can be determined from Figure 1 or from the two potential functions, is

$$\Delta W = 0.0021 \quad .$$

Since the variation in width of the potential function with energy can be determined from Figure 1, the value of K can be calculated and is

$$K = 1.210 \quad ,$$

and by Table I, n being three,

$$(n+\tfrac{1}{2})\frac{\omega_e'}{D_e'} = 0.1310 \quad .$$

Therefore the value of f is computed from Equation (15) to be

$$f = 0.98675 \quad .$$

Thus the second approximation to the true Morse potential function is

$$U_{(2)}(r-r_e') = 86,734.3\left(1 - e^{-2.2449(r-1.1506)}\right)^2 \quad .$$

The new energy levels become

$$E_n = 2135.46(n+\tfrac{1}{2}) - 13.144(n+\tfrac{1}{2})^2 \quad cm^{-1} \qquad (16)$$

In Figure 1 these energy levels are shown by the dashed lines along with second approximate potential.

The wave functions calculated from this second approximate potential should be very close to the true Morse potential wave functions, provided the value of r_e' is changed for each energy level so that the second approximate potential matches the true Morse potential at the energy level of the wave function concerned. The necessary change in r_e' required to match the approximate potential is given beside each energy level as Δr_e in Figure 1.

The wave functions for the excited states calculated by this approximate potential function may now be used with those from the ground state potential to evaluate the "over-lap integrals" in terms of the gamma function.

Formulas for Evaluation of the "Over-lap Integrals"

Designating quantities of the upper electronic state involved in the transition by a single prime and those for the lower electronic state by a double prime, the two sets of wave functions corresponding to Equation (5) become

$$\psi_n' = N_n' e^{-\frac{z'}{2}} (z')^{\frac{\beta'}{2}} F_n(z')$$
$$\psi_n'' = N_n'' e^{-\frac{z''}{2}} (z'')^{\frac{\beta''}{2}} F_n(z'') \qquad (17)$$

where $F_n(z)$ is by Equations (7) and (8)

$$F_0(z') = 1$$
$$F_1(z') = 1 - \frac{z'}{\beta_1' + 1}$$
$$F_2(z') = 1 - \frac{2z'}{\beta_2' + 1} + \frac{(z')^2}{(\beta_2'+1)(\beta_2'+2)}$$

$$F_3(z') = 1 - \frac{3z'}{(\beta_3'+1)} + \frac{3(z')^2}{(\beta_3'+1)(\beta_3'+2)} - \frac{(z')^3}{(\beta_3'+1)(\beta_3'+2)(\beta_3'+3)} \qquad (18)$$

and similarly for the ground state functions. Values of β_n are given by Equation (8) and N_n by Equation (9).

In order to evaluate the "over-lap integrals" z' must be expressed in terms of z''. By Equations (6) and (4)

$$z' = 2\alpha' Y' = 2\alpha' e^{-a''(r-r_e')}$$

$$z'' = 2\alpha'' Y'' = 2\alpha'' e^{-a''(r-r_e'')} \qquad a' = a''$$

Therefore,

$$z' = \left[\frac{\alpha'}{\alpha''} e^{-a''(r_e''-r_e')}\right] z''$$

As the value of r_e' varies with the vibrational energy level of the upper electronic state, the coefficient of z'' in the last equation will be a function of the energy level of the upper state. Therefore letting

$$\gamma_n = \frac{\alpha'}{\alpha''} e^{-a''(r_e''-r_e'(n))} \qquad , n = 0, 1, 2, \cdots \qquad (19),$$

then

$$z' = \gamma_n z'' \qquad (20)$$

Since the values of the "over-lap integrals" are to be evaluated relative to the two lowest vibrational wave functions, it is of value to determine the normalization

coefficients in terms of the normalization coefficients for the two lowest vibrational states. This can easily be done from Equation (12), with the aid of the well known gamma function formula

$$\Gamma(t+1) = t\Gamma(t) \quad . \tag{21}$$

Thus,

$$\begin{aligned}
N_0^2 &= N_o^2 \\
N_1^2 &= (2\alpha-2)^2(2\alpha-3)\,N_o^2 \\
N_2^2 &= \tfrac{1}{2}(2\alpha-2)(2\alpha-3)^2(2\alpha-4)^2(2\alpha-5)\,N_o^2 \\
N_3^2 &= \tfrac{1}{6}(2\alpha-2)(2\alpha-3)(2\alpha-4)^2(2\alpha-5)^2(2\alpha-6)^2(2\alpha-7)\,N_o^2 \\
N_4^2 &= \tfrac{1}{24}(2\alpha-2)\cdot\cdot\cdot\cdot\cdot \\
&\cdot\cdot\cdot\cdot\cdot\cdot
\end{aligned} \tag{22}$$

where α' is to be used for the upper electronic state and α'' for the ground electronic state.

Therefore by Equations (17), (18), (20), and (22) Equation (2), for the relative values of the "over-lap integrals", becomes

$$R_{v'v''} = \frac{\int_0^\infty \psi_{v'}\,\psi_{v''}\,dr}{\int_0^\infty \psi_o'\,\psi_o''\,dr}$$

$$= \frac{N_{v'}'\,N_{v''}''}{N_o'\,N_o''}\left\{\frac{\int_0^\infty e^{-\left(\frac{1+\gamma_{v'}}{2}\right)z''}\,\gamma_{v'}^{\frac{\beta_{v'}'}{2}}\,(z'')^{\frac{\beta_{v'}'+\beta_{v''}''}{2}-1}\,F_{v'}(z'')F_{v''}(\gamma_{v'}z'')\,dz''}{\int_0^\infty \gamma_o^{\beta_o'/2}\,e^{-\left(\frac{1+\gamma_o}{2}\right)z''}\,(z'')^{\frac{\beta_o'+\beta_o''}{2}-1}\,dz''}\right\}$$

.

By evaluating the integral in the denominator by the integral

formula

$$\int_0^\infty x^n e^{-ax}\, dx = \frac{\Gamma(n+1)}{a^{n+1}} \qquad (23)$$

it becomes

$$R_{v'v''} = \frac{N'_{v'} N''_{v''} \gamma_{v'}^{\frac{\beta'_{v'}}{2}} \left(\frac{1+\gamma_0}{2}\right)^{\frac{\beta'_0+\beta''_0}{2}}}{N'_0 N''_0 \gamma_0^{\beta''_0/2} \Gamma\left(\frac{\beta'_0+\beta''_0}{2}\right)} \int_0^\infty e^{-\left(\frac{1+\gamma_{v'}}{2}\right)z''} (z'')^{\frac{\beta'_{v'}+\beta''_{v''}}{2}-1} F_{v'}(z'') F_{v''}(\gamma_{v'} z'')\, dz''$$

Obviously, as $F_v(z)$ is a polynomial in z, the remaining integral can be evaluated by the same formula, Equation (23), in terms of the gamma function. Carrying this out for $v'=v''=0$ and $v'=v''=1$, one obtains

$$R_{00} = 1$$

$$R_{11} = \left\{ \frac{(2\alpha'-2)(2\alpha''-2)\left[(2\alpha'-3)(2\alpha''-3)\right]^{\frac{1}{2}} \left(\frac{1+\gamma_0}{2}\right)^{\alpha'+\alpha''-1} \gamma_1^{\alpha'-\frac{3}{2}}}{\gamma_0^{\alpha'-\frac{1}{2}} \Gamma(\alpha'+\alpha''-1)} \right\} \left\{ \frac{\Gamma(\alpha'+\alpha''-3)}{\left(\frac{1+\gamma_1}{2}\right)^{\alpha'+\alpha''-3}} \right.$$

$$- \frac{\Gamma(\alpha'+\alpha''-2)}{(2\alpha''-2)\left(\frac{1+\gamma_1}{2}\right)^{\alpha'+\alpha''-2}} - \frac{\gamma_1 \Gamma(\alpha'+\alpha''-2)}{(2\alpha'-2)\left(\frac{1+\gamma_1}{2}\right)^{\alpha'+\alpha''-2}}$$

$$\left. + \frac{\gamma_1 \Gamma(\alpha'+\alpha''-1)}{(2\alpha'-2)(2\alpha''-2)\left(\frac{1+\gamma_1}{2}\right)^{\alpha'+\alpha''-1}} \right\}$$

Applying Equation (21)

$$R_{11} = \left(\frac{\gamma_1}{\gamma_0}\right)^{\alpha'-\frac{1}{2}} \left(\frac{1+\gamma_0}{1+\gamma_1}\right)^{\alpha'+\alpha''-1} \frac{\left[(2\alpha'-3)(2\alpha''-3)\right]^{\frac{1}{2}}}{\frac{1}{2}\left[(2\alpha'-3)+(2\alpha''-3)\right]} \left\{ (\alpha'+\alpha''-3) - \frac{(2\alpha''-2)(\alpha'+\alpha''-3)}{\alpha'+\alpha''-2} \left(\frac{1+\gamma_1}{2}\right) \right.$$

$$\left. - \frac{(2\alpha'-2)(\alpha'+\alpha''-3)}{(\alpha'+\alpha''-2)\gamma_1} \left(\frac{1+\gamma_1}{2}\right) + \frac{(2\alpha'-2)(2\alpha''-2)}{(\alpha'+\alpha''-2)\gamma_1} \left(\frac{1+\gamma_1}{2}\right)^2 \right\}$$

Continuing in this manner, formulas can be obtained for all values of v', v'' that are desired. As can be seen, the formulas become extremely involved as one goes to higher vibrational quantum numbers. However they can be put in simplified form.

Defining

$$C_{mn} = \tfrac{1}{2}\left[(2\alpha'-m)+(2\alpha''-n)\right] \tag{24}$$

,

$$b_{mn} = \frac{1}{C_{mn}}\left[(2\alpha'-m)(2\alpha''-n)\right]^{\frac{1}{2}} \tag{25}$$

,

$${}^{v'v''}S_n'' = \frac{\left(\frac{1+\gamma_{v'}}{2}\right)(2\alpha''-n)}{\left[C_{nn}-(1+v'-v'')\right]} \tag{26}$$

,

$${}^{v'v''}S_n' = \frac{\left(\frac{1+\gamma_{v'}}{2}\right)(2\alpha'-n)}{\gamma_{v'}\left[C_{nn}-(1+v''-v')\right]} \tag{27}$$

,

$$h_{v'} = \left(\frac{\gamma_{v'}}{\gamma_0}\right)^{\alpha'-\frac{1}{2}}\left(\frac{1+\gamma_0}{1+\gamma_{v'}}\right)^{C_{11}} \tag{28}$$

,

the formulas for the "over-lap integrals", using the values of ${}^{v'v''}S_n$ as indicated by the subscripts on $R_{v'v''}$, become

$$R_{10} = h_1\,(2\alpha'-3)^{\frac{1}{2}}\,(S_2'-1) \tag{29}$$

$$R_{21} = h_2 b_{32} (2\alpha'-5)^{\frac{1}{2}} \frac{C_{23}}{C_{22}} \left\{ \sqrt{2}(S_3'-1) + \frac{C_{44}}{\sqrt{2}}(S_2''-1)(S_4'S_3'-2S_3'+1) \right\}$$

$$R_{32} = h_3 b_{22} b_{35} (2\alpha'-7)^{\frac{1}{2}} \frac{C_{35}}{C_{33}} \left\{ \sqrt{3}(S_4'-1) + \sqrt{3}\, C_{55}(S_4''-1)(S_4'S_5'-2S_4'+1) + \right.$$

$$\left. \frac{C_{55}C_{66}}{2\sqrt{3}} (S_5''S_4''-2S_5''+1)(S_6'S_5'S_4'-3S_5'S_4'+3S_4'-1) \right\}$$

$$R_{43} = h_4 b_{22} b_{33} b_{47} (2\alpha'-9)^{\frac{1}{2}} \frac{C_{47}}{C_{44}} \left\{ 2(S_5'-1) + 3C_{66}(S_5''-1)(S_6'S_5'-2S_5'+1) + \right.$$

$$C_{66}C_{77}(S_6''S_5''-2S_5''+1)(S_7'S_6'S_5'-3S_5'S_6'+3S_5'-1) +$$

$$\left. \frac{C_{66}C_{77}C_{88}}{12}(S_7''S_6''S_5''-3S_6''S_5''+3S_5''-1)(S_8'S_7'S_6'S_5'-4S_7'S_6'S_5'+6S_6'S_5'-4S_5'+1) \right\}$$

$$R_{54} = \begin{matrix} \cdot & \cdot & \cdot & \cdot \\ \cdot & \cdot & \cdot & \cdot \\ \cdot & \cdot & \cdot & \cdot \end{matrix}$$

$$R_{00} = 1$$

$$R_{11} = h_1 b_{33} \frac{C_{23}}{C_{22}} \left\{ 1 + C_{33}(S_2'-1)(S_2''-1) \right\}$$

$$R_{22} = h_2 b_{22} b_{55} \frac{C_{55}}{C_{33}} \left\{ 1 + 2C_{44}(S_3'-1)(S_3''-1) + \tfrac{1}{2} C_{44}C_{55}(S_3'S_4'-2S_3'+1)(S_4''S_3''-2S_3''+1) \right\}$$

$$R_{33} = h_3 b_{22} b_{33} b_{77} \frac{C_{77}}{C_{33}} \left\{ 1 + 3C_{55}(S_4'-1)(S_4''-1) + \tfrac{3}{2} C_{55}C_{66}(S_5'S_4'-2S_4'+1)(S_5''S_4''-2S_4''+1) + \right.$$

$$\left. \frac{C_{55}C_{66}C_{77}}{6} (S_6'S_5'S_4'-3S_5'S_4'+3S_4'-1)(S_6''S_5''S_4''-3S_5''S_4''+3S_4''-1) \right\}$$

$$R_{44} = h_4 b_{22} b_{33} b_{44} b_{99} \frac{C_{99}}{C_{55}} \Big\{ 1 + 4C_{66}(S_5'-1)(S_5''-1) + 3C_{66}C_{77}(S_6'S_5'-2S_5'+1)(S_6''S_5'' - 2S_5''+1) + \frac{2}{3} C_{66}C_{77}C_{88}(S_7'S_6'S_5' - 3S_6'S_5' + 3S_5' - 1)(S_7''S_6''S_5'' - 3S_6''S_5'' + 3S_5'' - 1) + \frac{1}{24} C_{66}C_{77}C_{88}C_{99}(S_8'S_7'S_6'S_5' - 4S_7'S_6'S_5' + 6S_6'S_5' - 4S_5' + 1)(S_8''S_7''S_6''S_5'' - 4S_7''S_6''S_5'' + 6S_6''S_5'' - 4S_5'' + 1) \Big\}$$

$$R_{55} = \begin{matrix} \cdot & \cdot & \cdot & \cdot \\ \cdot & \cdot & \cdot & \cdot \\ \cdot & \cdot & \cdot & \cdot \end{matrix}$$

$$R_{01} = (2\alpha''-3)^{\frac{1}{2}}(S_2''-1)$$

$$R_{12} = h_1 b_{32}(2\alpha''-5)^{\frac{1}{2}} \frac{C_{33}}{C_{22}} \Big\{ \sqrt{2}(S_3''-1) + \frac{C_{44}}{\sqrt{2}}(S_3'-1)(S_4''S_3'' - 2S_3''+1) \Big\}$$

$$R_{23} = h_2 b_{22} b_{35}(2\alpha''-7)^{\frac{1}{2}} \frac{C_{35}}{C_{33}} \Big\{ \sqrt{3}(S_4''-1) + \sqrt{3}\, C_{55}(S_4'-1)(S_5''S_4'' - 2S_4''+1) + \frac{1}{2\sqrt{3}} C_{55}C_{66}(S_5'S_4' - 2S_5'+1)(S_6''S_5''S_4'' - 3S_5''S_4'' + 3S_4'' - 1) \Big\}$$

$$R_{34} = h_3 b_{22} b_{33} b_{47}(2\alpha''-9)^{\frac{1}{2}} \frac{C_{47}}{C_{44}} \Big\{ 2(S_5''-1) + \cdot \quad \cdot \quad \cdot \Big\}$$

$$R_{45} = \begin{matrix} \cdot & \cdot & \cdot & \cdot \\ \cdot & \cdot & \cdot & \cdot \\ \cdot & \cdot & \cdot & \cdot \end{matrix}$$

Where desired, further formulas can be obtained by integrating the wave functions and simplifying. However one should be careful not to use wave functions of energy states of too high a quantum number since the Morse potential is not accurate for all ranges of energy. The formulas given above cover all the CN bands that will be measured in this experiment.

Evaluation of the "Over-lap Integrals" for the Violet CN System

Evaluation of the "over-lap integrals", and in turn the transition probabilities for the violet CN system by the equal amplitude approximation, requires a knowledge of the constants α', α'', C_{mn}, b_{mn}, $\overset{v'v''}{S}{}'_n$, $\overset{v'v''}{S}{}''_n$, $\gamma_{v'}$ and $h_{v'}$ as defined by Equations (6), (24), (25), (26), (27) and (28). These constants are necessary in order to evaluate Equations (29). Equation (6) can be put in more usable form for calculating α by substitution of Equation (11) and (12) for a and D_e; then Equation (6) becomes

$$\alpha = \frac{\omega_e}{2\omega_e x_e}$$

Now, by using the values of ω_e'' and $\omega_e'' x_e''$ given in Table I for the ground state X, and the values of ω_e' and $\omega_e' x_e'$ from Equation (16), as calculated from the second approximate potential function, the values of α'' and α' become

$$\alpha'' = \frac{\omega_e''}{2\omega_e'' x_e''} = 78.694$$

$$\alpha' = \frac{\omega_e'}{2\omega_e' x_e'} = 81.233$$

The value of γ_0 , defined by Equation (19), is obtained using the values of r_e'' and r_e' (for $n = 0$) given in Table I. Thus

$$\gamma_0 = 0.98428 \quad ,$$

and, as the variation in r_e' is very small,

$$\gamma_n = \gamma_0 \left(1 + 2.2448\, \Delta r_e'(n)\right) \qquad (30)$$

where $\Delta r_e'(n)$ is given in Figure 1. The four values of γ_n are given in Table II.

TABLE II

Values of γ_n

n	0	1	2	3	4
γ_n	0.98428	0.98645	0.99087	0.99619	0.99973

Using these values of α'' , α' and γ_n , the other constants are evaluated by substitution in Equations (24),(25), (26),(27) and (28), and are compiled in Tables III through XI.

The "over-lap integrals" as evaluated by Equations (29) are compiled in Table XII for the transitions measured in this experiment. Table XIII contains the relative transition probabilities, the squares of the values of the "over-lap integrals", as calculated by the equal amplitude approximation. For comparison, the values calculated by perturbation theory

by McKellar and Buscombe[13] are listed in parenthesis below the values obtained by the equal amplitude approximation. The two sets of values agree reasonably well for the very lowest quantum numbers but deviate considerably for quantum numbers of three or four. Perturbation theory calculations are known to become less accurate with the higher quantum numbers. For the equal amplitude approximation, however, the error should be reasonably constant in magnitude over the range of quantum numbers included in Table XIII since the amplitudes were matched at the third energy level, E_3, and the error in width at E_0 is too small to be observed in Figure 1. Thus the order of magnitude of the error in the equal amplitude approximation calculations of transition probabilities can be estimated by comparing the values for the 1-1 transition obtained by the two calculations. The difference is about 0.03 as seen in Table XIII. Therefore, the transition probabilities as calculated by the equal amplitude approximation should agree with experimental values within the range of ± 0.03. There may be a small additional error common to the two methods that results from the fact that CN is not a homonuclear molecule. However this latter error should be much smaller than 0.03.

TABLE III

Values of C_{mn}

n \ m	1	2	3	4	5	6	7	8	9
1	158.927								
2		157.927	157.427						
3		157.427	156.927		154.927				
4				155.927			154.427		
5			154.927		154.927				
6						153.927			
7							152.927		
8					154.427			151.927	
9									150.927

TABLE IV

Values of b_{mn}

n \ m	2	3	4	5	6	7	8	9
2	.99986							
3		.99986						
4			.99986					
5				.99986				
6					.99986			
7						.99986		
8							.99986	
9								.99986

TABLE V

Values of $^{v'v''}S_n'$, $v' = v'' + 1$

n \ v'	1	2	3	4
2	1.023018			
3		1.020868		
4		1.020973	1.018224	
5			1.018329	1.016523
6			1.018436	1.016629
7				1.016737
8				1.016846

TABLE VI

Values of $^{v'v''}S_n'$, $v' = v''$

n \ v'	1	2	3	4
2	1.029572			
3		1.027415		
4		1.027563	1.024796	
5			1.024945	1.023127
6			1.025095	1.023277
7				1.023429
8				1.023584

TABLE VII

Values of $^{v'v''}S_n'$, $v' = v'' - 1$

n \ v'	1	2	3
2	1.036175		
3		1.034047	
4		1.034238	1.031453
5			1.031647
6			1.031842
7			
8			

TABLE VIII

Values of ${}^{v'v''}S_n''$, $v''= v'+1$

n \ v'	0	1	2	3
2	.976187			
3		.977148		
4		.977095	.979229	
5			.979124	.981731
6			.979018	.981624
7				.981517
8				.981408

TABLE IX

Values of ${}^{v'v''}S_n''$, $v'=v''$

n \ v'	1	2	3	4
2	.9834772			
3		.98561277		
4		.98554934	.98817301	
5			.98810859	.98986089
6			.98804332	.98979550
7				.98972925
8				.98966213

TABLE X

Values of ${}^{v'v''}S_n''$, $v''= v'-1$

n \ v'	2	3	4
2	.99199678		
3		.99461533	
4		.99459276	.99635656
5			.99633365
6			.99631044
7			
8			

TABLE XI

Values of $h_{v'}$

v'	0	1	2	3	4
$h_{v'}$	1	1.00407	1.01183	1.02005	1.02489

TABLE XII

Values of $|R_{v'v''}|$

v' \ v''	0	1	2	3	4
0	1	.296			
1	.292	.921	.399		
2		.374	.876	.441	
3			.388	.859	.452
4				.416	.843

TABLE XIII

Values of $R^2_{v'v''}$

v' \ v''	0	1	2	3	4
0	1 (1)	.088 (.095)			
1	.085 (.091)	.848 (.822)	.159 (.169)		
2		.140 (.161)	.767 (.662)	.194 (.244)	
3			.151 (.212)	.737 (.538)	.204 (.305)
4				.173 (.252)	.711

III. MEASUREMENT OF RELATIVE TRANSITION PROBABILITIES

Preliminary

The measurements of the transition probabilities of the CN violet band system is to be carried out by comparing the peak intensities of each band head with the intensity of the $\lambda\lambda$ 3883.4 band head, 0-0 transition. Before this can be accomplished the rotational structure of the bands must be investigated to determine what corrections are necessary to allow for the slightly different rotational structure of the individual bands.

The violet band system of CN is a $^2\Sigma - ^2\Sigma$ transition, where $^2\Sigma$ is the ground state of the molecule. In this type of transition the rotational lines are doublets. However, the doublet splitting is so small that even with spectrographs of the highest resolving power the splitting is not observed until high rotational quantum numbers are reached. Therefore, the lines of these bands can be treated as singlets; in fact they are often cited in text books as an example of singlet bands.[14] Thus the wave number distribution of the rotational lines of these bands can be represented by the well known formula[15] for singlet transitions. For the CN violet system, where the band heads are formed in the P branch $(\Delta J = -1)$, this is

$$\nu = \nu_0 + (B'_{v'} + B''_{v''})J - (B'_{v'} - B''_{v''})J^2 \qquad (31)$$

where $\nu \equiv$ wave number of rotational line in cm^{-1},

$\nu_0 \equiv$ wave number of orgin of band,

$J \equiv$ rotational quantum number of lower state

involved in the transition,

$B'_{v'} \equiv$ constant inversely proportional to the moment of inertia of the molecule in the upper electronic state with vibrational quantum number v',

$B''_{v''} \equiv$ constant inversely proportional to the moment of inertia of the molecule in the lower electronic state with vibrational quantum number v''.

Location of Band Heads

The location of the head of the band is determined from Equation (31) by the value of J for which the first derivative of the equation with respect to J is zero; that is

$$\frac{\partial \nu}{\partial J} = (B'_{v'} + B''_{v''}) - 2(B'_{v'} - B''_{v''})J_h = 0$$

where J_h is the value of J at the band head. Thus the value of the rotational quantum at the band head is given by

$$J_h = \frac{B'_{v'} + B''_{v''}}{2(B'_{v'} - B''_{v''})} \quad . \tag{32}$$

Since the values of $B''_{v''}$ and $B'_{v'}$ differ for different vibrational states, the value of J_h will be different for each band. The effect of this on the vibrational transition probabilities determined from observations of band head intensities must be considered, especially when comparing bands of different sequences.

The variation of B_v with vibrational state of the

molecule is approximately linear and can be represented by the formula

$$B_v = B_e - \alpha_e (v + \tfrac{1}{2})$$

where $B_e \equiv$ the equilibrium value of the rotational constant,

$B_v \equiv$ the value of the rotational constant in the state with vibrational quantum number v,

$\alpha_e \equiv$ constant coupling the vibration and rotation of the molecule.

The values of B_e and α_e for the two states concerned are shown in Table XIV part of which is taken from Herzberg.[16] These constants are determined by fitting the observed wave numbers of the rotational lines to Equation (31) or equations derived from it. Usually the rotational lines used in this evaluation of B_e and α_e are rotational lines whose J quantum number is quite different from the J_h quantum number given by Equation (32) because of the difficulty in analyzing the overlapping rotational lines forming the band head. Smit-Miessen[2] has made an accurate analysis of the rotational structure near the band head of the 0-0 and 1-1 CN bands. The constants he obtained by fitting his results to an equation similar to Equation (32) are slightly different than those given in Herzberg which represent an average value over all the CN violet bands. Values of B_e and α_e calculated from Smit-Miessen's data are also shown in Table XIV.

TABLE XIV

Values of B_e and α_e

	Herzberg		Smit-Miessen	
State	B_e	α_e	B_e	α_e
B	1.9701	0.02215	1.96948	0.021095
X(Ground)	1.8996	0.01735	1.90008	0.017805

While the difference in the two values of B_e is quite negligible, the two values of α_e differ enough to cause differences in the computed values of the quantum numbers of the lines at the band heads. Because the values of B_e and α_e given by Herzberg represent an average value for all the CN bands being measured in this experiment, Smit-Miessen's values being for the 0-0 and 1-1 bands only, Herzberg's values will be used in the calculation of constants quoted in this thesis. Values of J_h are given in Table XV.

It will be noted that the values of J_h computed by Equation (32) are not integers. However, since the peak of the band heads is the sum of a number of rotational lines, this number is significant; it represents the average J_h quantum number at the band head.

Relative Number of Rotational Lines in the Band Head

Another important factor affecting the determination of vibrational transition probabilities from band head intensity measurements is the number of rotational lines blended at the band head to give the resultant peak intensity. Since the value of J_h is different for each band, these numbers

TABLE XV

Values of J_n

ν'/ν''	0	1	2	3	4
0	28.267	22.426			
1	41.649	30.098	23.516		
2		46.030	32.230	24.743	
3			51.566	34.743	26.137
4				58.784	37.750

will also be different.

If the range in wave numbers over which the rotational lines are added together to form the band head is $\Delta\nu$, and the corresponding range in J values is ΔJ, Equation (31) can be written:

$$\nu + \Delta\nu = \nu_0 + (B'_{v'} + B''_{v''})(J + \Delta J) - (B'_{v'} - B''_{v''})(J + \Delta J)^2$$

with the aid of Equation (32). $\Delta\nu$ and ΔJ for the band head are related by

$$\Delta\nu = -(B'_{v'} - B''_{v''})(\Delta J)^2$$

and

$$\Delta J = \pm\sqrt{\frac{|\Delta\nu|}{|B'_{v'} - B''_{v''}|}}$$

The measurements have been carried out on the one meter, concave grating spectrograph at the Mount Wilson Observatory Laboratory. This spectrograph has an almost constant dispersion in wave length over the range of the violet CN bands being measured. Therefore since

$$\frac{\Delta\nu}{\nu} = -\frac{\Delta\lambda}{\lambda}$$

or

$$\Delta\nu = -\frac{\Delta\lambda}{\lambda^2}\,10^8 = -\frac{(\text{constant})^2}{\lambda^2} \quad ,$$

$$\Delta J = \pm\frac{(\text{constant})}{\lambda_h}\sqrt{\frac{1}{|B'_{v'} - B''_{v''}|}}$$

where λ_h is the wave length of the band head considered. Obviously the number ΔJ affects the intensity of the band heads as a statistical weight, representing the number of rotational lines involved in the measurement. Even though the value of the constant in Equation (33) is not known, the relative values of ΔJ can be computed from the known values of $\lambda_h, B''_{v''}$ and $B'_{v'}$. The values of ΔJ are given in Table XVI in terms of

$$S_{v'v''} = \frac{\lambda_h(v',v'')}{\text{CONSTANT}} \Delta J(v',v'') \quad .$$

Relative Intensities of the Band Heads

The information calculated above permits one to predict the relative intensities of the band heads of the CN violet system in terms of the vibrational transition probabilities and known constants when the spectrum is emitted under conditions of thermal equilibrium.

The intensity in emission of a vibrational transition in a band system is given by the formula

$$I_{v'v''} = N'_{v'} \nu^4 R^2_{v'v''}$$

where $N'_{v'}$ is the number of molecules in the upper electronic state with vibrational quantum number v', $R^2_{v'v''}$ is the transition probability, and ν is the frequency of the emitted radiation. In a source of excitation where conditions of thermal equilibrium prevail, relative values of $N'_{v'}$ for different vibrational states in the upper electronic level are given by the Boltzman formula; that is

$$N'_{v'} = N_o e^{-\frac{E_{v'}}{KT}}$$

TABLE XVI

Values of $S_{\mu\nu}$

μ/ν	0	1	2	3	4
0	3.832	3.321			
1	4.665	3.975	3.421		
2		4.830	4.134	3.631	
3			5.245	4.315	3.752
4				5.630	4.422

where N_o is the number of molecules in the ground state, $E_{v'}$ is the energy of vibration in the upper state, having vibrational quantum number J', K is Boltzmann's constant, and T is the absolute temperature. Thus the relative intensities of vibrational bands emitted under conditions of thermal equilibrium are given by

$$I_{v'v''} = N_o \nu^4 R^2_{v'v''} e^{-\frac{E_{v'}}{KT}} \quad . \tag{34}$$

This formula can not be used to compute relative intensities of band heads, however, even when the values of $R^2_{v'v''}$ are known, unless the effects of intensity variations due to rotational structure at the band heads being compared areso small as to be negligible. For CN this is not true as is indicated by Tables XV and XVI, and therefore, in order to use Equation (34), corrections for the variation in the structure of the band heads must be determined.

The variation of intensity in the rotational structure of the vibrational bands of diatomic molecules has been investigated and reliable formulas have been developed for most known types of electronic transitions. In the case of CN, where the rotational lines can be considered as singlets (although they are really unresolved doublets), the relative intensities of lines in a P branch emitted under thermal equilibrium are given by[11]

$$I_J = J e^{-\frac{E_R}{KT}} = J e^{-\frac{B'_v J(J-1)hc}{KT}}$$

where J is the rotational quantum number that is used in Equation (31), E_R is the energy of rotation of the molecule in the upper electronic state, and the other constants are the same as in Equation (31). Thus if the intensities of the fictitious lines at the band heads of each band could be compared, the relative intensities of the bands would be given by

$$I_{v'v''} = N_o \nu^4 R^2_{v'v''} J_h(v',v'') e^{-\frac{1}{KT}(E'_{v'} + E'_R)} \qquad (35)$$

However, what is measured at the band head is not the intensity of a single rotational line, but the sum of the intensities of a number of lines. Thus the relative intensities of the band heads are given by Equation (35) after it has been multiplied by the number of lines in the band head, that is, by the quantity ΔJ as defined by Equation (33). The relative intensities of the band heads observed with a spectrograph having constant dispersion are given then by

$$I_{v'v''} = N_o \nu^4 R^2_{v'v''} J_h(v',v'') \Delta J(v',v'') e^{-\frac{1}{KT}(E'_{v'} + E'_R)}$$

For intensities measured relative to the 0-0 band head and when R^2_{oo} is taken as unity, the intensity of a band, $v'-v''$, relative to the 0-0 band is

$$I_{v'v''} = \left(\frac{\nu(v',v'')}{\nu(0,0)}\right)^4 R^2_{v'v''} \frac{J_h(v',v'')}{J_h(0,0)} \frac{\Delta J_h(v',v'')}{\Delta J_h(0,0)} e^{-\frac{1}{KT}(E'_{v'} + E'_R - E'_o - E'_R(o))}$$

In terms of wave length and with the notation used in Table XVI this becomes

$$I_{v'v''} = R^2_{v'v''} \left(\frac{\lambda(0,0)}{\lambda(v',v'')}\right)^5 \frac{J_h(v',v'')}{J_h(0,0)} \frac{S_{v'v''}}{S_{oo}} e^{-\frac{1}{KT}(E'_{v'} + E'_R(v') - E'_o - E'_R(0))}$$

where the values of

$J_h(v';v'')$ are given in Table XV,

$S_{v'v''}$ are given in Table XVI, and

$E'_{v'}$ are given by the Equation (9),

$$E_R(v') = hc\, B'_{v'}\, J_h(v';v'')\,(J_h(v';v'') - 1) \quad .$$

Taking the logarithm of both sides of Equation (36) and transposing,

$$\log_{10}\left[\left(\frac{\lambda(0,0)}{\lambda(v';v'')}\right)^5 \frac{J_h(v';v'')}{J_h(0,0)}\ \frac{S_{v'v''}}{S_{00}} R^2_{v'v''}\right] = \log_{10} I_{v'v''} + \frac{\log_{10} e}{KT}\,(E'_{v'} + E'_R(v') - E'_o - E'_R(0))$$

Designating the coefficients of $R^2_{v'v''}$ as one constant,

$$C_{v'v''} = \left(\frac{\lambda(0,0)}{\lambda(v';v'')}\right)^5 \frac{J_h(v';v'')}{J_h(0,0)}\ \frac{S_{v'v''}}{S_{00}} \quad ,$$

and designating the difference in energy of the upper electronic states

$$\Delta E_{v'v''} = \frac{1}{hc}\,(E'_{v'} + E'_R(v') - E'_o - E'_R(0)) \quad ,$$

then the logarithms of the relative intensities are related to the transition probabilities by

$$\log_{10} C_{v'v''} R^2_{v'v''} = \log_{10} I_{v'v''} + \frac{hc \log_{10} e}{KT}\,\Delta E_{v'v''} \quad , \qquad (37)$$

where the values of $C_{v'v''}$ have been tabulated in Table XVII and the values $\frac{hc \log_{10} e}{K}\Delta E_{v'v''}$ are tabulated in Table XVIII. $E'_R(v')$ and $E'_{v'}$ have been computed from

$$E'_R(v') = B'_{v'}\, J_h(v';v'')\,(J_h(v';v'') - 1)$$

and

$$E'_{v'} = \omega'_e\,(v' + \tfrac{1}{2}) - \omega'_e x'_e\,(v' + \tfrac{1}{2})^2 \quad .$$

TABLE XVII

Values of $C_{v'v''}$

v'/v''	0	1	2	3	4
0	1	.456			
1	2.655	1.117	.504		
2		3.057	1.265	.573	
3			3.730	1.436	.637
4				4.572	1.607

TABLE XVIII

Values of $\frac{hc}{k} \log_{10} e \ \Delta E_{v'v''}$

v'/v''	0	1	2	3	4
0	0	-365.1			
1	2362.8	1395.7	961.9		
2		3909.9	2776.4	2322.8	
3			5490.2	4144.6	3635.2
4				7125.5	5503.1

Therefore, using these relationships and the appropriate constants, the values of $C_{v'v''}R^2_{v'v''}$ can be determined from measurements of the relative intensities of the band heads at different temperatures, and in turn the relative transition probabilities, $R^2_{v'v''}$, can be computed.

Technique of Measurement

Appearance of CN Bands:

The CN bands appear in emission from the electric furnace when the furnace is heated to a temperature in excess of 2200° K. There is ample nitrogen left in the furnace after evacuation to pressures of a few millimeters of Hg to form the CN. The amount of CN in the furnace varies greatly with temperature.

Determining the True Band Contours:

The measurements must be made so as to allow comparison of the intensities of the band heads. While in principle this appears simple, actually it is complicated by several factors. The first difficulty one encounters is that most of the band heads are not isolated but are blended with overlapping rotational lines of the P and R branches of the other bands. Therefore it is necessary to substract the effect of rotational lines of these other bands from the band head being measured. Frequently the peak intensity of these lines is many times that of the band head.

The intensity measurements in this experiment are carried out on photographic film by conventional methods which will be described later. As intensities add directly on photographic film, the effect of extraneous rotational

lines on a band head being measured can be considered as background radiation, and the intensity of these extraneous rotational lines along with the background radiation can be subtracted from the peak intensity at the band head provide the correct contour can be drawn in for the background of rotational lines. Figure 2 is a microphotometer tracing of the $\lambda\lambda$ 3883.4 band sequence with the band heads of the 0-0, 1-1 and 2-2 transitions labeled. A survey of this figure will indicate why allowance for the effect of overlapping rotational lines blended with the band heads is quite difficult. Several questions arise;

1. Does the band head of the 1-1 band coincide with the peak of a rotational line of the 0-0 band and if so, should line A-A represent the background to be used?
2. Is the band head located on the steep slope of one of the rotational lines of the 0-0 band and, therefore, should some average value, say B-B, be used for the background?
3. Is the band head of the 1-1 band located between the rotational lines of the 0-0 band and, therefore, should line C-C be used?
4. Is it possible that the change in population of the rotational levels of the 1-1 band with temperature can shift the location of the peak of the 1-1 band slightly with temperature so that all three of the above methods should be used depending on the

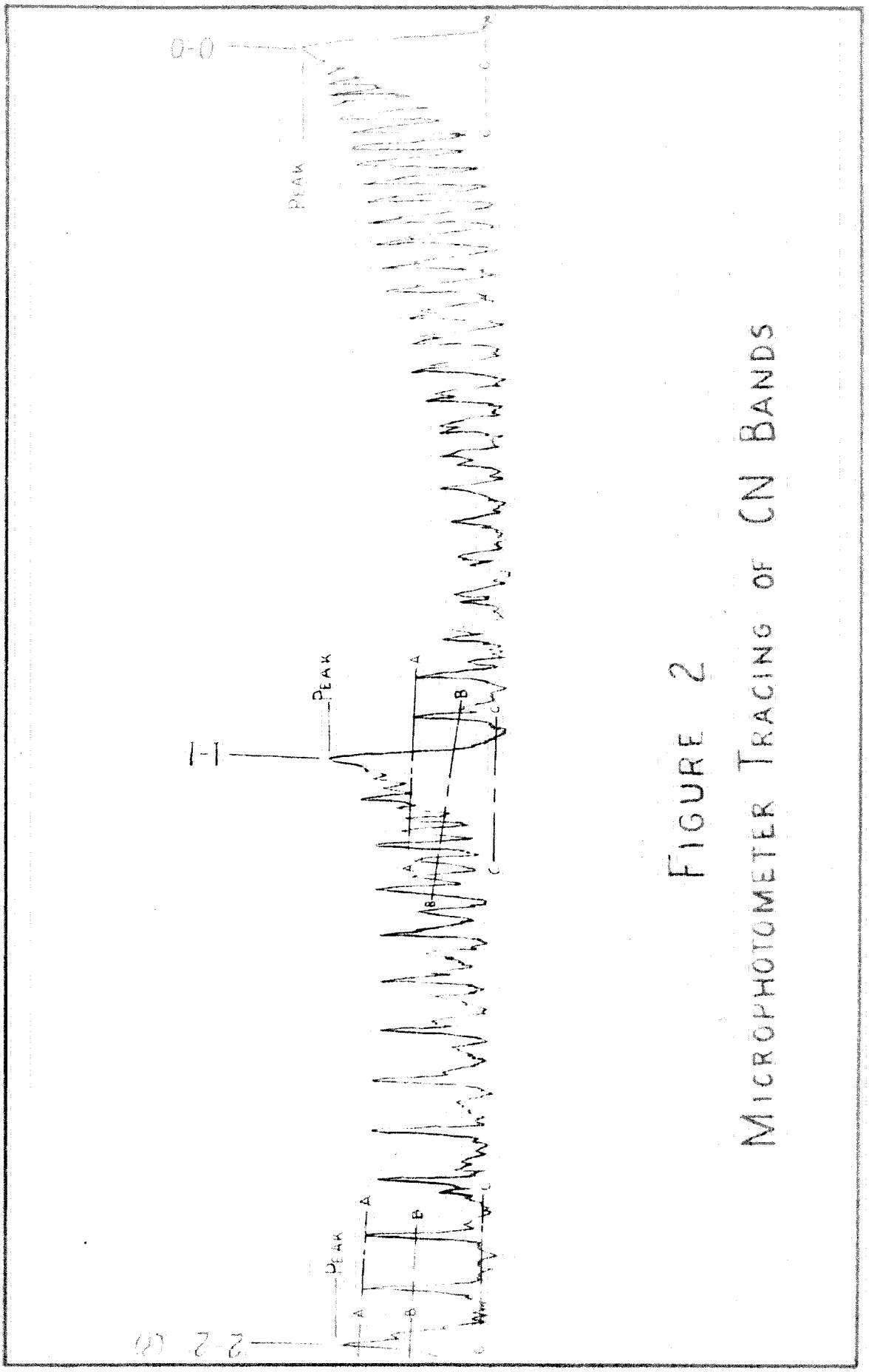

FIGURE 2

MICROPHOTOMETER TRACING OF CN BANDS

temperature at which the intensities are being measured?

These questions concerning the 1-1 band head will obviously also arise for all the band heads being measured except for the first member of each sequence.

A number of measurements were carried out on the relative intensities of the band heads at various temperatures using the three suggested methods of drawing in the background, and using combinations of them. The logarithms of the relative intensities measured by the various methods were plotted against the reciprocal of absolute temperature at which they were measured. These plots were then examined to determine which method would give results consistent with Equation (37).

The results were quite poor and the fluctuation in the individual measurements was so large that accurate determination of the variation of relative intensity with temperature was not possible. In fact, the apparent change in relative intensities with temperature was sometimes in the opposite direction to that predicted by Equation (37). However, the sequence beginning with 0-1 band head at 4216 A gave fairly consistent results by all three methods, although the variation of intensity with temperature was somewhat large.

While a number of different attempts were made to reduce the errors in the measurements of relative intensities of the band heads, only one of these gave satisfactory results. The slit width of the spectrograph was increased,

thereby broadening the individual rotational lines and reducing their peak intensities as compared to the band head peak intensity. The peak intensities of the band heads are little affected by widening the slit because of the fact that even with a narrow slit the band head is made up of many lines blended together and covering a relatively broad wave length range, and widening the slit has the effect of adding more rotational lines to the head to form the peak. With the one-meter spectrograph a slit width of between 30 and 50 microns made the band heads quite prominent as compared with the overlapping rotational lines of other bands and permitted a fairly precise determination of the background due to these lines. This process greatly reduced the scatter of measured intensities as a function of temperature, but the results were still not consistent with Equation (37). This inconsistency could not be attributed to the method of determining background and therefore no further attempts were made to improve the technique of measuring background.

Photographic Photometry:

The film used in the measurements was Eastman Panatomic-X. It was calibrated with the aid of a rotating sector with five openings each differing from the next in width by a factor of two. To avoid possible errors due to reciprocity law failure, etc., the band heads themselves were used to establish the characteristic curves of the emulsion. This was accomplished by placing the sector at the horizontal stigmatic focus of the spectrograph and forming an enlarged image of the far end of the furnace tube on the sector.

Each spectrogram then consisted of five strips differing in intensity in steps by a factor of two corresponding to the sector openings. Thus each photograph of the spectrum provided its own calibration. Figure 3 shows a typical spectrogram and Figure 4 is a microphotometer tracing giving the calibration curves of this spectrogram. The illumination of the sector by the image of the end of the furnace tube departed slightly from uniformity at the edges and appropriate corrections were made for this in plotting relative intensities.

To obtain the relative intensities of the band heads from a microphotometer tracing of a spectrogram, a plot is made of transmission against the logarithm of the relative intensity for each strip of spectrum given by the sector, the measurements being made at the band head peaks. The relative intensities of the band heads are then obtained from the displacements of the curves for different bands from a reference curve at 50% transmission. In a similar manner the intensity of the background (overlapping bands and continuum) at each band which must be subtracted from the band head intensity is determined. The intensity plots obtained from the calibration curves shown in Figure 4 are shown in Figure 5. The film was calibrated heterochromatically for the three sequences measured by means of the black body radiation from the electric furnace.

Several advantages of this method are evident. First, the intensity plots each consist of the average of several individual measurements of transmission. Second, the wide

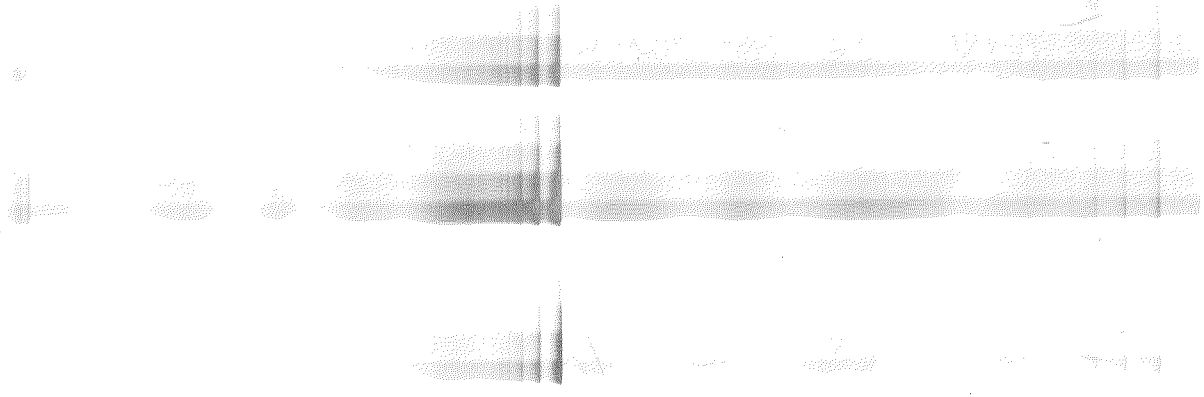

FIGURE 3
CALIBRATION SPECTROGRAM OF CN BANDS

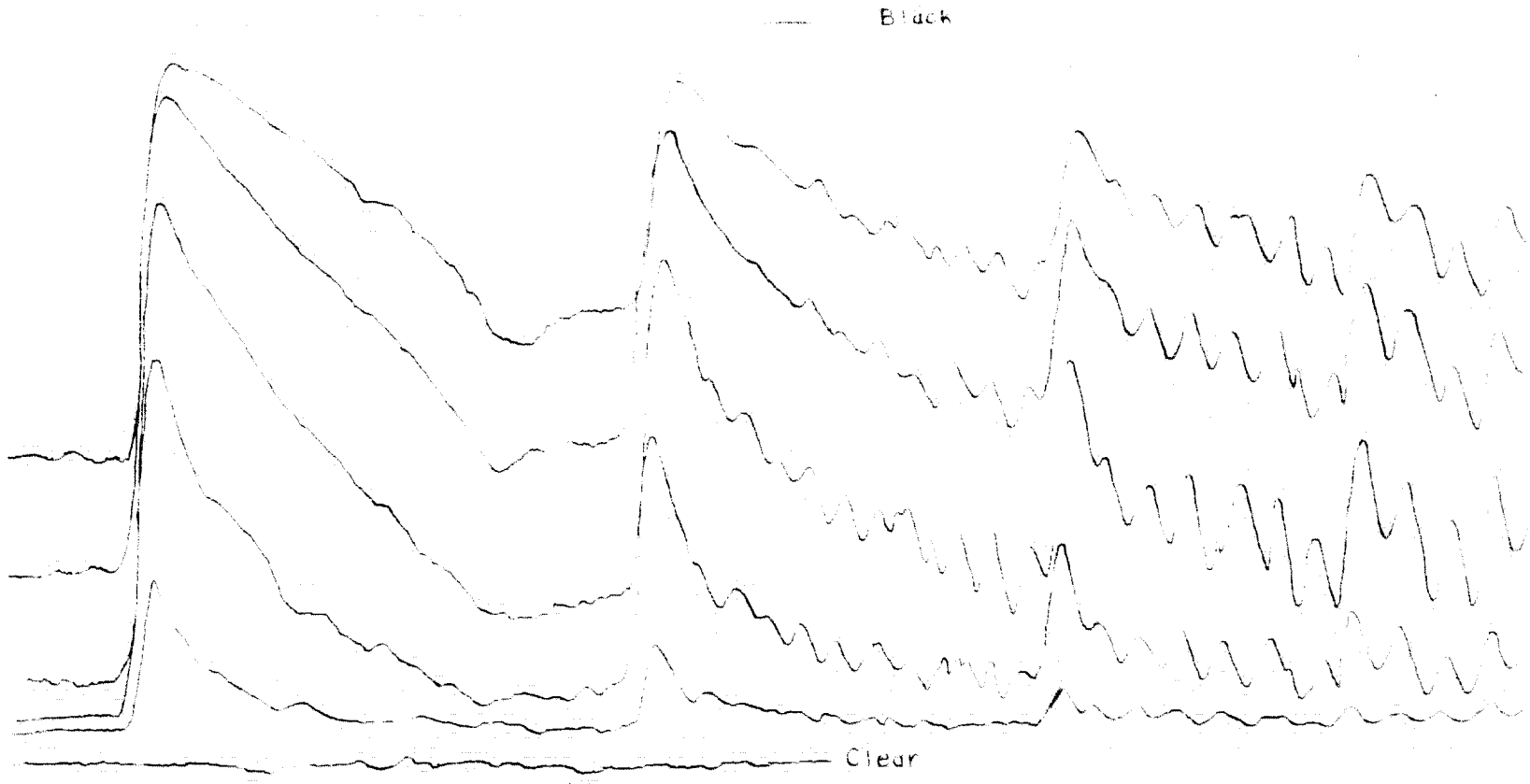

FIGURE 4

CALIBRATION CURVES FOR CN BANDS

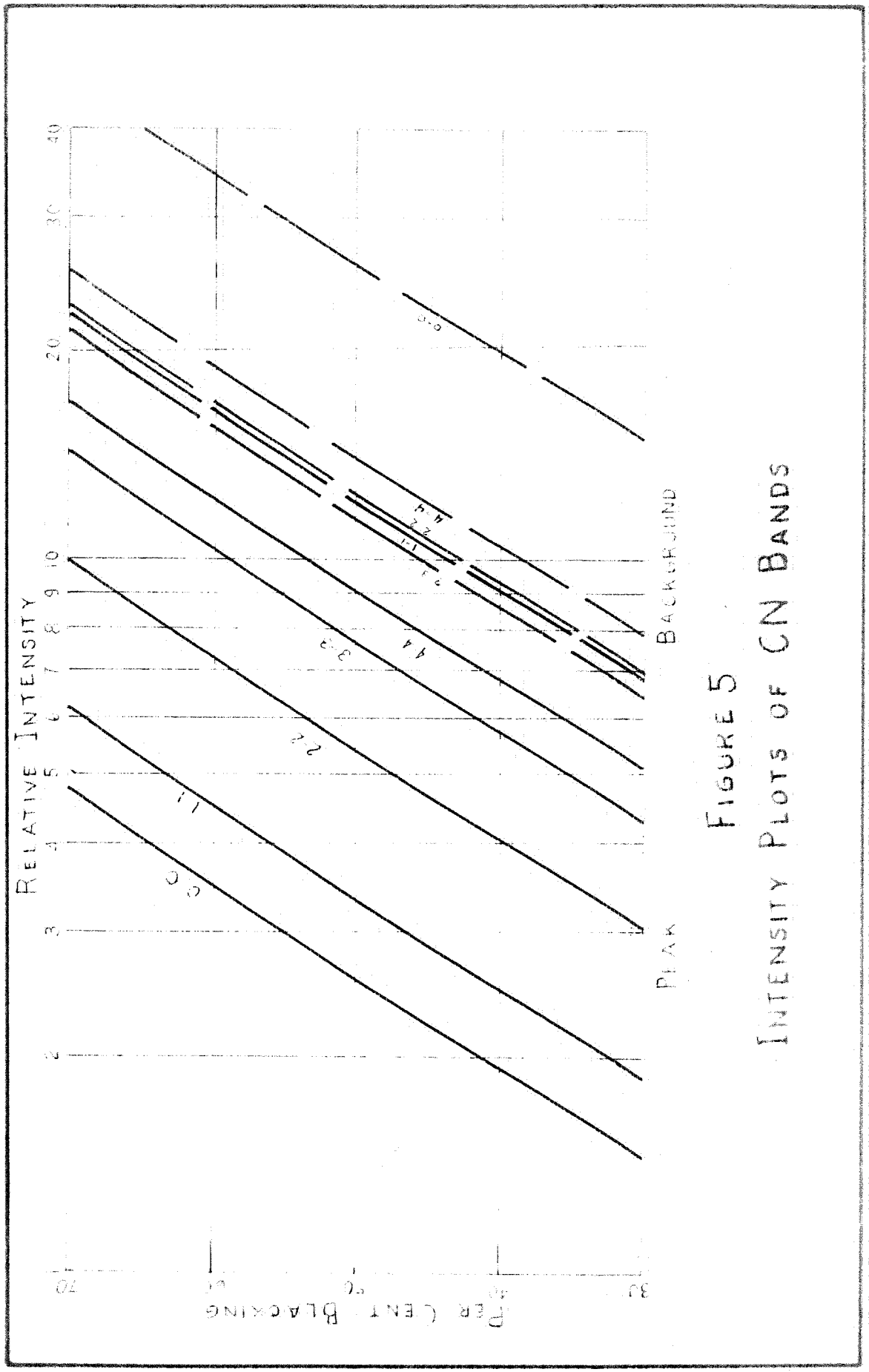

Figure 5

Intensity Plots of CN Bands

range in intensities of the strips due to the sector permit bands of widely different intensities to be measured on the same spectrogram. Third, the range in intensity of the strips permits a far more satisfactory determination of the background intensity than could be obtained from a single exposure.

Elimination of Reversal Effects:

Measurements of relative intensities of the band heads of CN made prior to development of the method described above for determining the true band contours indicated strong reversal effects. In an attempt to understand and to reduce these effects, an experiment, described in detail in Appendix 1, was carried out in which helium was blown down the tube of the furnace in the opposite direction in which the light traveled to the spectrograph. This tended to eliminate the cooler reversing layers of CN at the mouth of the furnace tube. The experiment described in Appendix 1 indicated that while this did not eliminate all of the reversing effects, it did reduce them and therefore for all subsequent measurements helium was passed through the furnace tube at the highest velocity possible without removing pieces of carbon from the tube when the furnace was operated at high temperatures. This flow rate was around four liters per minute. It is felt that this flow of helium eliminated "self reversal" from cooler layers and that the remaining reversal was due to "self absorption" by the CN gas in temperature equilibrium with the furnace.

Figure 6 is a plot of the logarithms of relative

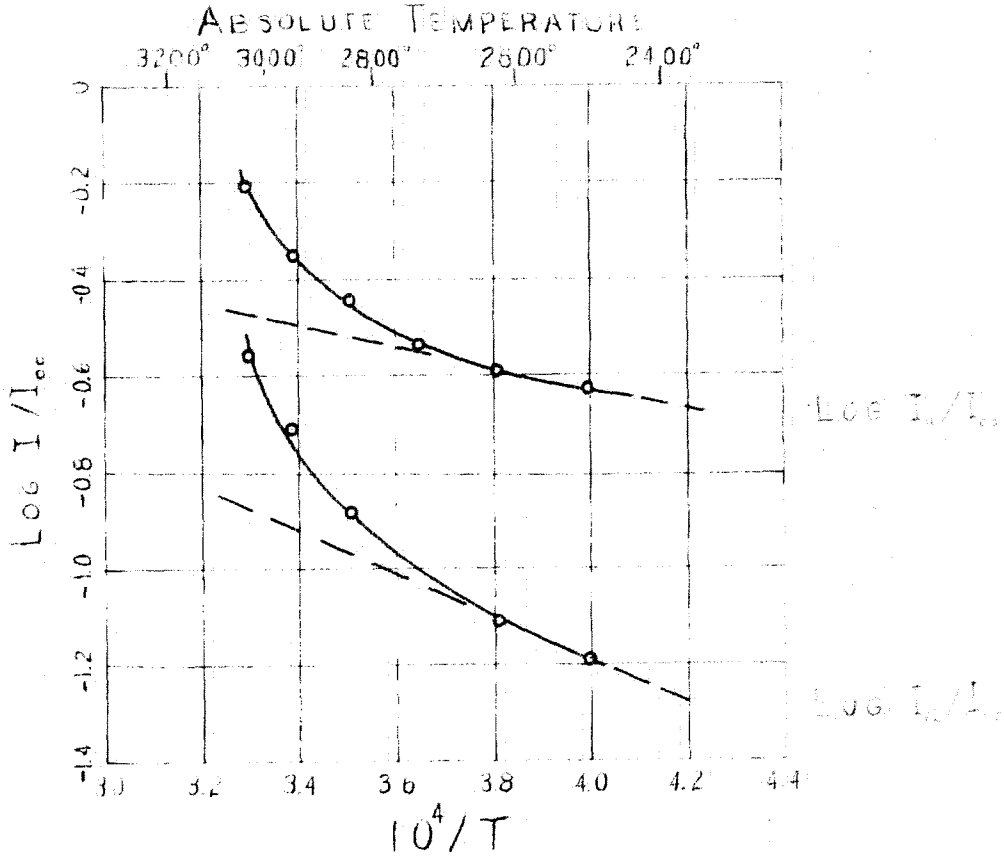

FIGURE 6

LOGARITHM OF RELATIVE INTENSITY VS INVERSE ABSOLUTE TEMPERATURE OF CN BANDS

intensities of two bands vs the inverse absolute temperature. The straight dashed lines represent the variations of relative intensities given by Equation 37. The effect of self absorption is to make the relative intensities of the weaker bands too large (when intensities are taken relative to the ground state transition as they are in Figure 6) because the 0-0 band is absorbed more than the 1-1 and 2-2 bands. The magnitude of the self absorption increases with temperature because the concentration of CN increases with temperature.

Fortunately, since the measurements of relative intensity are being carried out on a gas which is in thermal equilibrium with the walls of a furnace and since cooler reversing layers have been removed, information concerning self absorption by the bands emitted by the gas can be obtained. The peak intensity of a spectral line emitted under the conditions described above has been shown to be related to the true peak intensity of the spectral line by the equation[17]

$$I_e = I_p \left(1 - e^{-I_T/I_p}\right) \qquad (38)$$

where I_e is the peak emitted intensity of the line,
I_p is the Planck radiation intensity that exists in the furnace, and
I_T is the true intensity of the spectral line.

This equation can not be used to obtain the true intensity from measured values of I_e as the spectrograph does not measure the true peak emitted intensity of the spectral

line but measures intensities that are proportional to the peak emitted intensity. However, the above formula can be used to eliminate self absorption effects when these are small. Expanding Equation (38) and keeping only the first two terms one obtains

$$I_e = I_p\left(\frac{I_T}{I_p} - \frac{1}{2}\left[\frac{I_T}{I_p}\right]^2\right)$$

or

$$I_e = I_T\left(1 - \frac{1}{2}\frac{I_T}{I_p}\right) \quad .$$

Since I_e is proportional to I_m, the measured value of the relative intensity is

$$I_m = k I_e = k I_T\left(1 - \frac{1}{2}\frac{I_T}{I_p}\right) \quad .$$

Taking intensities relative to the 0-0 band this becomes

$$I_{mR}(v',v'') = \frac{I_m(v',v'')}{I_m(0,0)} = \frac{I_T(v',v'')}{I_T(0,0)}\left(\frac{1 - \frac{1}{2}\frac{I_T(v',v'')}{I_p(v',v'')}}{1 - \frac{1}{2}\frac{I_T(0,0)}{I_p(0,0)}}\right)$$

where $I_{v'v''} = \dfrac{I_T(v',v'')}{I_T(0,0)}$, the relative intensity appearing in Equation (37). Solving for $I_{v'v''}$ one obtains

$$I_{v'v''} = I_{mR}(v',v'')\left(\frac{1 - \frac{1}{2}\frac{I_T(0,0)}{I_p(0,0)}}{1 - \frac{1}{2}\frac{I_T(v',v'')}{I_p(v',v'')}}\right) \quad .$$

Taking the logarithm of both sides this becomes

$$\log_{10} I_{v'v''} = \log_{10} I_{mR}(v',v'') + \log_{10}\left(1 - \frac{1}{2}\frac{I_T(0,0)}{I_p(0,0)}\right) - \log_{10}\left(1 - \frac{1}{2}\frac{I_T(v',v'')}{I_p(v',v'')}\right) \quad .$$

If $I_T(v',v'')/I_p(v',v'')$ is small, this can be put in a more convenient form. Expanding the last two terms, one obtains:

$$\log_{10} I_{v'v''} = \log_{10} I_{mR}^{(v'v'')} + \frac{1}{2}\left(\frac{I_T(0,0)}{I_p(0,0)} - \frac{I_T(v'v'')}{I_p(v'v'')}\right) . \qquad (39)$$

If all measurements of relative peak intensities are on the same scale, $I_T(v'v'')$ may be replaced, with sufficient accuracy for this second order approximation, by

$$I_T(v'v'') = \frac{k'}{t} I_m(v'v'')$$

where k' is a constant (unknown),

t is exposure time on photographic film, and

$I_m^{(v'v'')}$ is measured relative intensity.

Thus Equation (39) becomes

$$\log_{10} I_{v'v''} = \log_{10} I_{mR}^{(v'v'')} + \frac{k'}{2t}\left(\frac{I_m(0,0)}{I_p(0,0)} - \frac{I_m(v'v'')}{I_p(v'v'')}\right) . \qquad (40)$$

Substituting this value of $\log_{10} I_{v'v''}$ in Equation (37), one obtains

$$\log_{10} C_{v'v''} R^2_{v'v''} = \left[\log_{10} I_{mR}^{(v'v'')} + \frac{hc}{KT}\log_{10} e \ \Delta E^{(v'v'')}\right] + \frac{k'}{2t}\left(\frac{I_m(0,0)}{I_p(0,0)} - \frac{I_m(v'v'')}{I_p(v'v'')}\right) .$$

The quantity in the brackets represents the apparent value of $\log_{10} C_{v'v''} R^2_{v'v''}$ if no absorption were considered. This may be defined as,

$$\log_{10}\left(C_{v'v''} R^2_{v'v''}\right)_a = \log_{10} I_{mR}^{(v'v'')} + \frac{hc}{KT}\log_{10} e \ \Delta E^{(v'v'')} .$$

The true value of $\log_{10} C_{v'v''} R^2_{v'v''}$ is related to the apparent value by the equation

$$\log_{10} C_{v'v''} R^2_{v'v''} = \log_{10} (C_{v'v''} R^2_{v'v''})_a + \frac{k'}{2t}\left(\frac{I_m^{(0,0)}}{I_p^{(0,0)}} - \frac{I_m^{(v',v'')}}{I_p^{(v',v'')}}\right) . \qquad (41)$$

Thus one may obtain the true values of $\log_{10} C_{v'v''} R^2_{v'v''}$ by calculating from measured relative intensities at different temperatures the values of $\log_{10}(C_{v'v''} R^2_{v'v''})_a$, plotting these latter values against the corresponding values of

$$\Delta\left(\frac{I_m}{I_p}\right) = \frac{1}{t}\left(\frac{I_m^{(0,0)}}{I_p^{(0,0)}} - \frac{I_m^{(v',v'')}}{I_p^{(v',v'')}}\right)$$

and performing a straight line extrapolation to the zero value of $\Delta\left(\frac{I_m}{I_p}\right)$. The values of $R^2_{v'v''}$ are then obtained with the aid of Table XVII.

Results of Measurements

Figures 7, 8, and 9 are plots of the values of log $\log_{10}(C_{v'v''} R^2_{v'v''})_a$ vs $\Delta\left(\frac{I_m}{I_p}\right)$ for the sequences of bands measured in this experiment. For the higher vibrational transitions of the $\Delta J = -1$ and $\Delta J = +1$ sequences values of $\log_{10}(C_{v'v''} R^2_{v'v''})_a$ were taken relative to the leading band head of the sequence, that is the 1-0 and 0-1 band heads respectively. The values of $\log_{10}(C_{v'v''} R^2_{v'v''})_a$ plotted on Figures 7, 8, and 9 were extrapolated to zero values of $\Delta\left(\frac{I_m}{I_p}\right)$ to give true relative values of $\log_{10} C_{v'v''} R^2_{v'v''}$. These values of $\log_{10} C_{v'v''} R^2_{v'v''}$ were then all reduced to the same scale, relative to the 0-0 band. Finally, using values of $C_{v'v''}$

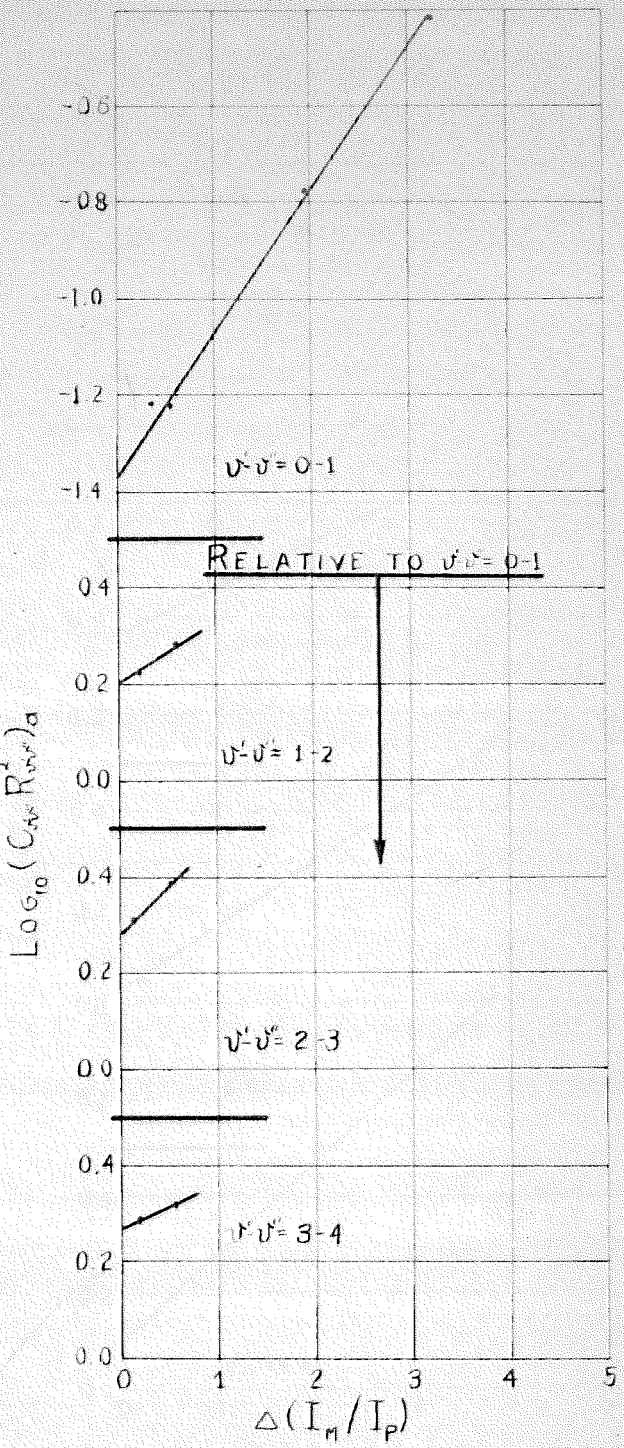

FIGURE 7

LOG $(C_{v'v''}R^2_{v'v''})_a$ PLOTS FOR $\Delta v = -1$ SEQUENCE

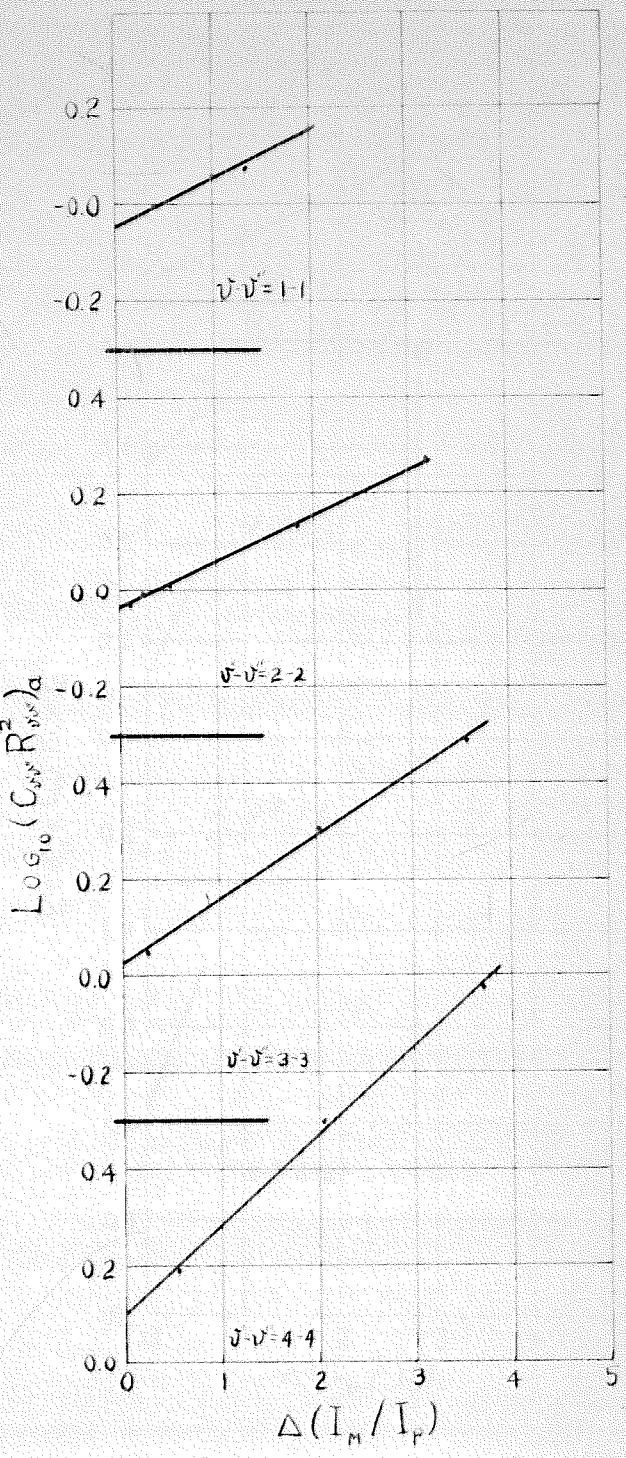

FIGURE 8

LOG $(C_{v'v''}R^2_{v'v''})_a$ PLOTS FOR $\Delta v = 0$ SEQUENCE

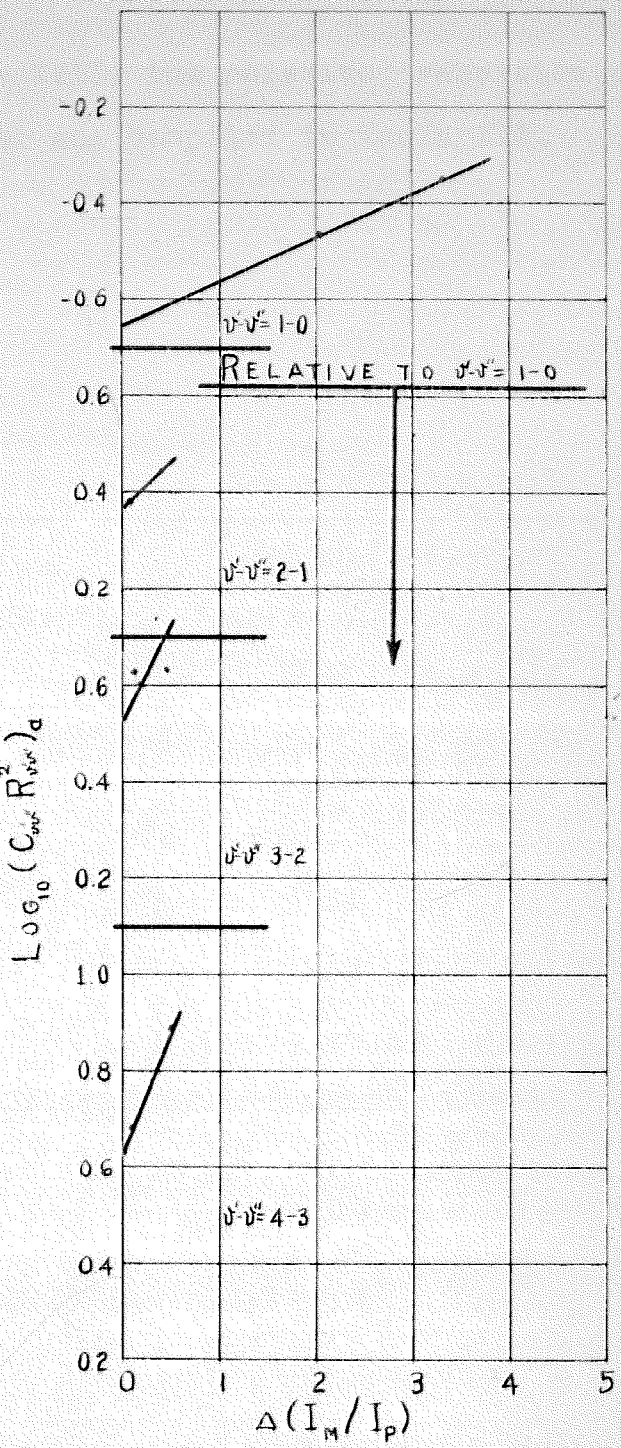

FIGURE 9

LOG $(C_{v'v''}R^2_{v'v''})_a$ PLOTS FOR $\Delta J = +1$ SEQUENCE

given in Table XVII, the relative transition probabilities were determined and compiled in Table XIX.

TABLE XIX

Measured Values of Relative

Transition Probabilities, $R^2_{v'v''}$

v'/v''	0	1	2	3	4
0	1	.092			
1	.083	.813	.133		
2		.165	.736	.141	
3			.194	.732	.124
4				.204	.776

IV. COMPARISON OF RESULTS

The relative transition probabilities measured in the present experiment have been assembled in Table XX for comparison with the values calculated by the equal amplitude approximation. The average deviation of calculated relative transition probabilities from measured values is 0.001. The differences between calculated relative transition probabilities and measured relative transition probabilities are within the limits of accuracy of the calculations and of the measurements.

In the calculation, errors might be introduced by: (a) neglecting the variation of the electric moment of the molecule with internuclear distance, (b) neglecting interaction of rotation and vibration on relative transition probabilities, and (c) using the equal amplitude approximation only for the upper level potential function. The equal amplitude approximation could have been improved by matching the width of the approximate potential function at each energy level. However, the error introduced by matching only at the third energy level is probably within the accuracy of the Morse potential function for this electronic energy level.

In the measurements slight errors might be introduced by (a) the inability to accurately determine the average J_h quantum number at the band head, (b) the inability to determine exactly the relative number of rotational lines blended in the band heads, (c) the linear extrapolation to eliminate self absorption, and (d) possible slight non-

TABLE XX

Comparison of $R^2_{v'v''}$ Values

Calculated by the Equal

Amplitude Approximation with

Measured Values

$v'-v''$	Calculated	Measured	Difference
0-1	.088	.092	.004
1-2	.159	.133	-.026
2-3	.194	.141	-.053
3-4	.204	.124	-.080
0-0	1	1	0
1-1	.848	.813	-.035
2-2	.767	.736	-.031
3-3	.737	.732	-.005
4-4	.711	.776	.065
1-0	.085	.083	-.002
2-1	.140	.165	.025
3-2	.151	.194	.043
4-3	.173	.205	.032

uniformity in the temperature along the length of the furnace tube. Because of these possible systematic errors, the agreement between theory and experiment is believed to be well within the limits of the experiment, even though the differences between calculated and measured transition probabilities are greater than the random fluctuations of the measurements.

Relative transition probabilities calculated by perturbation theory from the paper of McKellar and Buscombe[12] are given in Table XXI for comparison with the measured values. The agreement here is very good for the transitions of very low quantum numbers, but differences become quite large for larger values of vibrational quantum numbers.

TABLE XXI

Comparison of $R^2_{v'v''}$ Values

Calculated by Second Order

Perturbation Theory with

Measured Values

$v'-v''$	Calculated	Measured	Difference
0-1	.095	.092	-.003
1-2	.169	.133	-.036
2-3	.244	.141	-.103
3-4	.305	.124	-.181
0-0	1	1	0
1-1	.822	.813	-.009
2-2	.662	.736	.074
3-3	.538	.732	.194
4-4		.776	
1-0	.091	.083	-.008
2-1	.161	.165	.004
3-2	.212	.194	-.018
4-3	.252	.205	-.047

V. CONCLUSIONS

The agreement of the calculated and experimental values of the relative vibrational transition probabilities of the CN violet band system determined in this investigation indicate the following:

(a) The experimental technique for measuring relative vibrational transition probabilities from low dispersion band head data, developed for this work, is satisfactory for the CN violet band system. In principle, the technique can be extended to bands which arise from more complicated electronic transitions than a $^2\Sigma - {}^2\Sigma$ transition.

(b) The new theoretical treatment, the equal amplitude approximation, is reliable for the CN violet band system and yields more accurate results for the higher vibrational transitions than previous existing approximations. In principle, theoretical vibrational transition probabilities for band systems in other homonuclear or near homonuclear molecules can be computed by the equal amplitude approximation.

(c) If relative transition probabilities are known, the experimental technique developed in this investigation can be used to determine temperature from measured values of relative intensity if self absorption effects are removed or allowed for.

Several precautions should be observed in using experimental band head intensity data. Care must be taken

to be sure that absorption effects have been removed from band head peak intensities. Because of the high concentration of radiation at the peaks of the band heads, self absorption is much greater at the peak than for rotational lines in the band which are capable of being resolved, ie., those whose true widths (by Doppler, natural, or collision damping) are less than their separations. Sum rules should not be applied to band head intensity measurements unless the various effects of the rotational structure in the band head have first been properly allowed for. This is especially important when the measurements are to be used to determine the temperature of the radiating source. Also, extreme care must be taken to eliminate the effects of over-lapping rotational structure on the band heads.

REFERENCES

1. Brinkman, H., Thesis, Utrecht, (1937).

2. Smit-Miessen, M. M. and Spiers, J. L., Physica 9 193 (1942).

3. Smit, J. A. and Spires, J. L., Physica 9 597 (1942).

4. Herzberg, G., Molecular Spectra and Molecular Structure I. Spectra of Diatomic Molecules p 200 eq 73 (D. Van Nostrand Company New York, N. Y. 1951).

5. King, A. S., Ap. J. 56, 318 (1922).

6. Hutchisson, E., Phys. Rev. 36, 410 (1930).

7. Hutchisson, E., Phys. Rev. 37, 45 (1931).

8. Schiff, L. I., Quantum Mechanics p 178-87 (McGraw-Hill Book Company, Inc., New York, N. Y. (1949).

9. Herzberg, G. Ibid p 196.

10. Morse, P. M., Physi. Rev. 34, 57 (1929).

11. Wu, Ta-You, Vibrational Spectra and Structure of Polyatomic Molecules p 51 (China Science Corporation, Shanghi, 1939).

12. Herzberg, G., Ibid, p 520

13. McKellar and Buscombe, Pub. Dom. Ap. Obs., Victoria Vol. 7, No. 23, (1948).

14. Herzberg, G., Ibid, p 42

15. Herzberg, G., Ibid, p 205 eq. IV 80

16. Harrison, G. R., Lord, R. C., and Loofbourow, J. R., Practical Spectroscopy p 326-361 (Prentice Hall, New York, N. Y. 1948).

17. Smit, J. A., Physica 12, 683 (1946).

APPENDIX I

INVESTIGATION OF SELF REVERSAL OF VIOLET CN BANDS

At the time of this experiment a satisfactory method of determining the background effects of the overlapping rotational structure on band heads had not been developed. The effect of the overlapping rotational structure on the variation of relative intensity with temperature is quite small as compared with that for the variation of relative intensity of the vibrational structure. Therefore, even though measured relative intensities may contain systematic errors due to drawing in the background intensity incorrectly, the variation of relative intensity with temperature should still follow the course predicted by Equation (37).

Because it had been observed that the variation of measured relative intensity vs inverse of absolute temperature was much larger, especially for the $\Delta v = 0$ sequence, than would be expected from Equation (37), it was believed that this reversal might result from cooler layers of CN gas at the mouth of the furnace tube. Therefore, in order to remove these cooler layers, and at the same time decrease the concentration of CN, the end of the furnace tube nearer the spectrograph, was fitted with a quartz window. An inlet was provided at this window so that helium could be blown down the furnace tube in the opposite direction to that which the light traveled to the spectrograph. Since the gas was being removed from the furnace at a constant volume pumping rate, the concentration of CN in the furnace tube should then be almost inversely proportional

to the helium flow rate down the furnace tube.

Measurements of relative intensity of the CN bands vs temperature for three different flow rates (2, 4, 6 liters per minute) of helium were carried out. The results of these measurements are given in Table XVII and Figure 10. Figure 10 is a plot of logarithms of relative intensities for the three band heads, 1-1, 2-2, 3-3 relative to 0-0, vs inverse of temperatures at the three flow rates of helium. As can be seen, the effect of helium flow rate on the slopes of these plots is quite marked between the flow rates of two and four liters per minute.

For three values of inverse temperature, 3.8×10^{-4}, 3.6×10^{-4}, 3.4×10^{-4}, the values of logarithms of relative intensities were plotted against the inverse of flow rate and extrapolated to zero as shown in Figure 11. These extrapolated values are plotted in Figure 12. The dashed lines in Figure 12 represent the slopes predicted by Equation (37).

The results of this experiment indicate that:

1. Part of the self reversal effects are removed by blowing helium down the furnace tube.
2. The slopes of the plots of logarithm of relative intensity vs inverse of temperature probably can not be made to agree with theory for any flow rate of helium.

Therefore it was decided to carry out all future experiments at helium flow rates of four liters per minute, which would

eliminate the major self reversal effects probably due to cooler layers of CN.

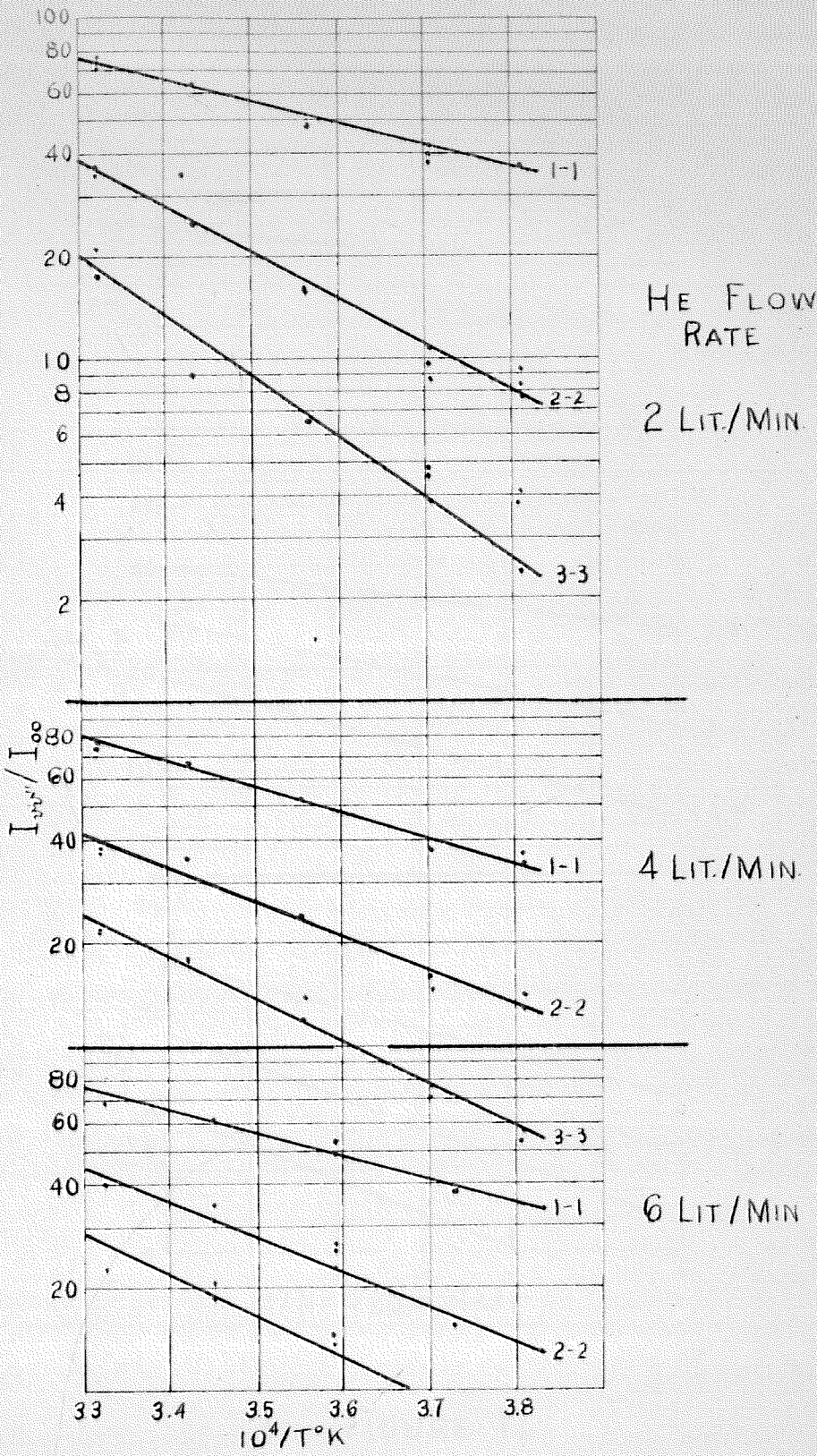

Figure 10

Intensity Plots of CN Band Heads, $\Delta J=0$

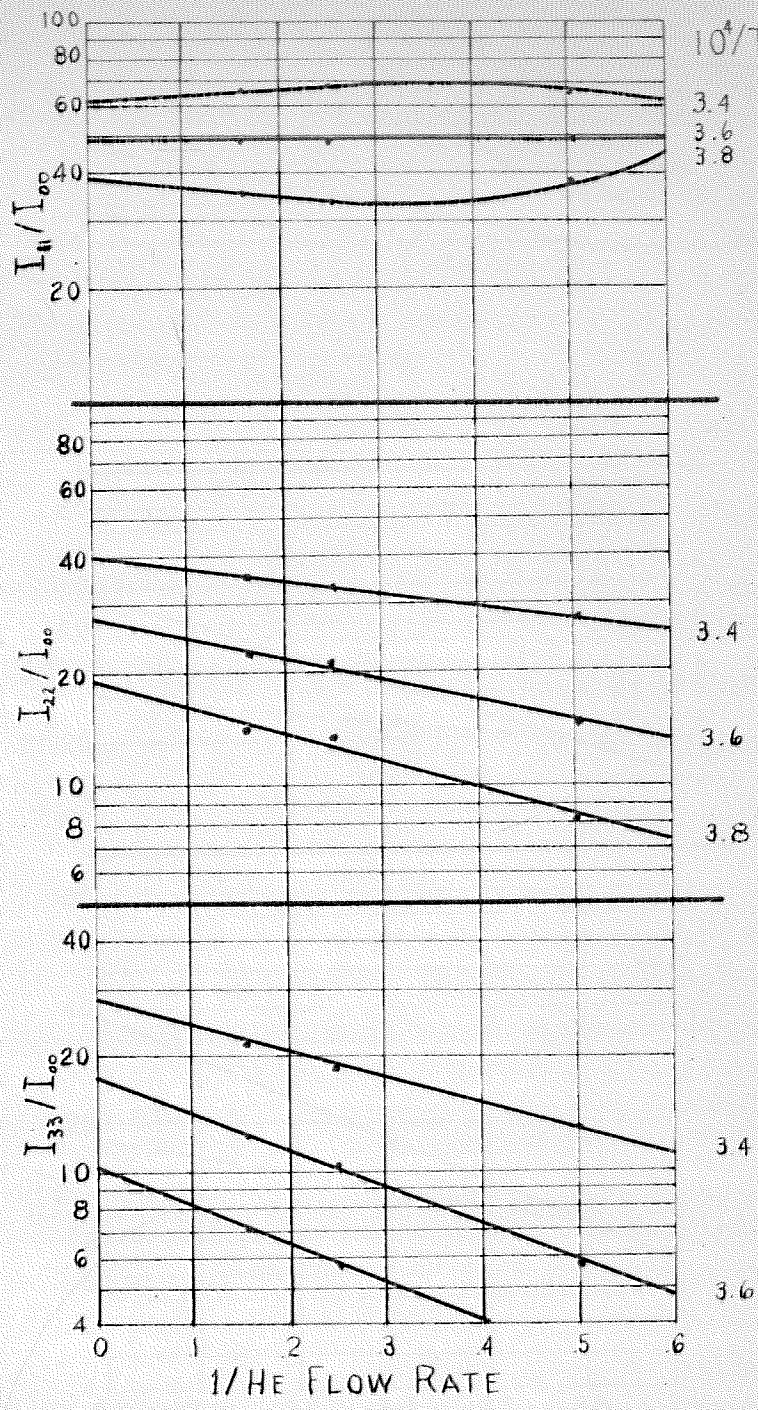

FIGURE 11

EXTRAPOLATION OF RELATIVE INTENSITIES

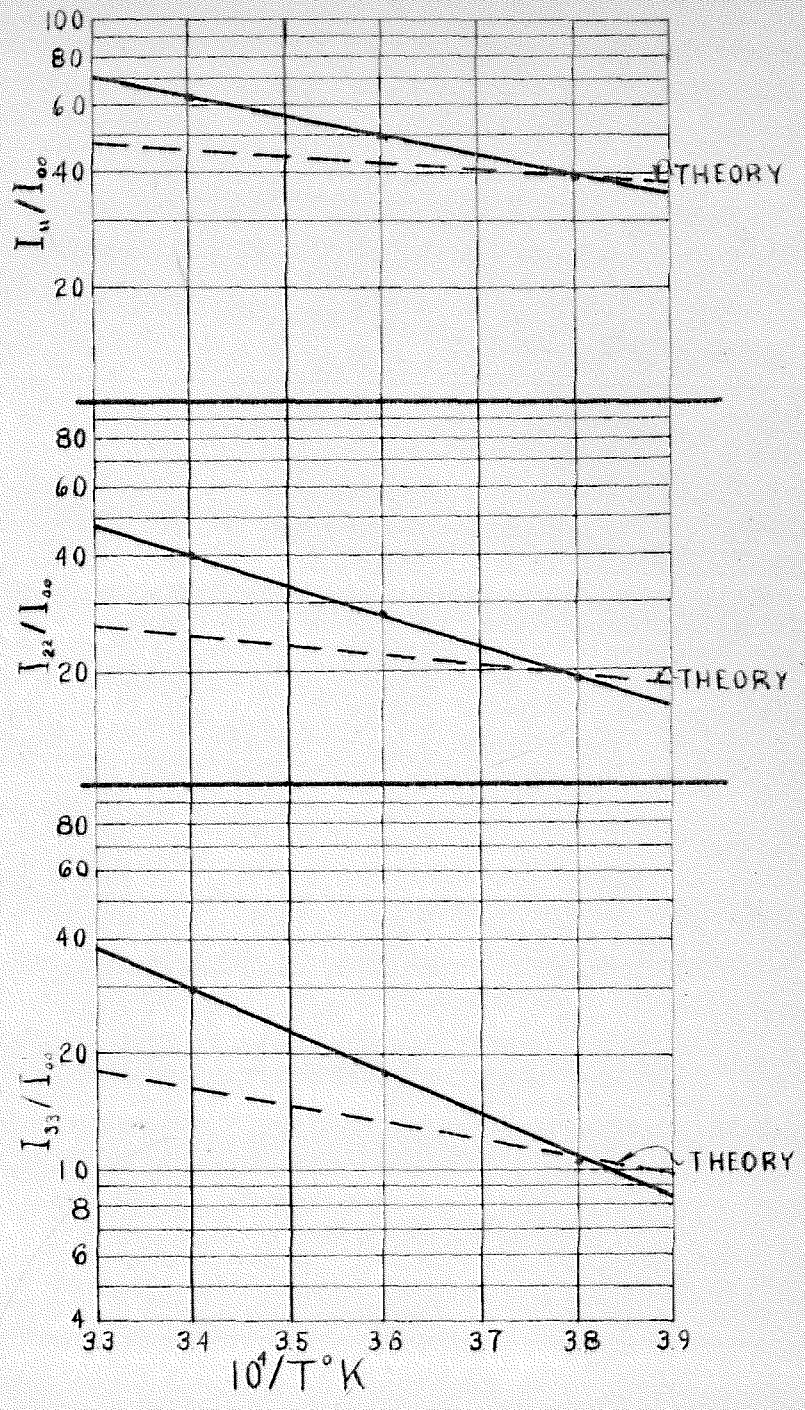

FIGURE 12

EXTRAPOLATED RELATIVE INTENSIY PLOTS